

UNIVERSIDAD DE CONCEPCIÓN



CENTRO DE INVESTIGACIÓN EN
INGENIERÍA MATEMÁTICA (CI²MA)



On entropy stable schemes for degenerate parabolic
multispecies kinematic flow models

RAIMUND BÜRGER, PAUL E. MÉNDEZ,
CARLOS PARÉS

PREPRINT 2018-24

SERIE DE PRE-PUBLICACIONES

ON ENTROPY STABLE SCHEMES FOR DEGENERATE PARABOLIC MULTISPECIES KINEMATIC FLOW MODELS

RAIMUND BÜRGER^A, PAUL E. MÉNDEZ^A, AND CARLOS PARÉS^B

ABSTRACT. Entropy stable schemes for the numerical solution of initial value problems of nonlinear, possibly strongly degenerate systems of convection-diffusion equations were recently proposed in [S. Jerez, C. Parés, *Entropy stable schemes for degenerate convection-diffusion equations*, SIAM J. Numer. Anal. vol. 55 (2017) pp. 240–264]. These schemes extend the theoretical framework by [E. Tadmor, *The numerical viscosity of entropy stable schemes for systems of conservation laws. I*, Math. Comp. vol. 49 (1987) pp. 91–103] to convection-diffusion systems. They arise from entropy conservative schemes by adding a small amount of viscosity to avoid spurious oscillations. It is demonstrated that this formulation can naturally be extended to initial-boundary value problems with zero-flux boundary conditions in one space dimension, including an explicit bound on the growth of the total entropy. The main condition for feasibility of entropy conservative or stable schemes for a given model is that the corresponding first-order system of conservation laws possesses a convex entropy function and corresponding entropy flux, and that the diffusion matrix multiplied by the inverse of the Hessian of the entropy is positive semidefinite. These assumptions are satisfied by certain diffusively corrected multiclass kinematic flow models of arbitrary size that describe traffic flow or the settling of dispersions and emulsions, where the latter application gives rise to zero-flux boundary conditions. Numerical examples illustrate the behavior and accuracy of entropy stable schemes for these applications.

1. INTRODUCTION

1.1. **Scope.** This work concerns numerical schemes for systems of degenerate convection-diffusion equations in one space dimension of the form

$$\mathbf{u}_t + \mathbf{f}(\mathbf{u})_x = (\mathbf{K}(\mathbf{u})\mathbf{u}_x)_x, \quad x \in I \subset \mathbb{R}, \quad t \in \mathbb{R}_+, \quad (1.1)$$

where $I = \mathbb{R}$ or I is a bounded interval, $\mathbf{u} = (u_1, \dots, u_N)^\top : I \times \mathbb{R}_+ \rightarrow \Omega \subset \mathbb{R}^N$ is the vector of unknown functions of position x and time t , $\mathbf{f} = (f_1, \dots, f_N)^\top$ is a given flux vector, and $\mathbf{K}(\mathbf{u}) \in \mathbb{R}^{N \times N}$ is a semipositive definite diffusion matrix defined in Ω . We allow that $\mathbf{K}(\mathbf{u}) = \mathbf{0}$ on a set of \mathbf{u} -values of positive N -dimensional measure, so (1.1) is, in general, strongly degenerate. Equation (1.1) is equipped with the initial condition

$$\mathbf{u}(x, 0) = \mathbf{u}_0(x), \quad x \in I; \quad (1.2)$$

Date: May 10, 2018.

2010 *Mathematics Subject Classification.* 35L65, 65L06, 65M20, 76T20.

Key words and phrases. degenerate convection-diffusion equations, entropy stable schemes, polydisperse sedimentation, multiclass traffic flow.

^ACI²MA and Departamento de Ingeniería Matemática, Facultad de Ciencias Físicas y Matemáticas, Universidad de Concepción, Casilla 160-C, Concepción, Chile. E-Mail: rburger@ing-mat.udec.cl, pmendez@ing-mat.udec.cl.

^BDepartamento de Análisis Matemático, Facultad de Ciencias, Universidad de Málaga, Campus de Teatinos s/n, E-29071 Málaga, Spain. E-Mail: pares@uma.es.

if I is bounded, that is $I = [0, L]$ with $L > 0$, then we impose, in addition, the zero-flux boundary condition

$$(\mathbf{f}(\mathbf{u}) - \mathbf{K}(\mathbf{u})\mathbf{u}_x)|_{x=0} = \mathbf{0}, \quad (\mathbf{f}(\mathbf{u}) - \mathbf{K}(\mathbf{u})\mathbf{u}_x)|_{x=L} = \mathbf{0}. \quad (1.3)$$

For the problem (1.1), (1.2), whose solutions are in general discontinuous, Jerez and Parés [1] devised so-called entropy stable finite difference schemes. These schemes extend the concept of entropy stable methods for systems of conservation laws due to Tadmor [2]. Such schemes capture correctly the appearance and propagation of shocks but may induce strong oscillations close to them, so some artificial viscosity needs to be added in such a way that the resulting numerical becomes entropy stable (i.e., the entropy satisfies a system of differential inequalities arising from a spatially discrete but continuous in time entropy inequality). It was shown in [1] that a necessary condition for such a method to be feasible for (1.1) is that the first-order system of conservation laws

$$\mathbf{u}_t + \mathbf{f}(\mathbf{u})_x = \mathbf{0} \quad (1.4)$$

has a convex entropy function $\eta = \eta(\mathbf{u})$ and entropy flux $g = g(\mathbf{u})$, for which the entropy inequality

$$\eta(\mathbf{u})_t + g(\mathbf{u})_x \leq 0$$

is valid (in the sense of distributions) for solutions of (1.4) [3]. It is well known that for $N \geq 3$, the existence of an entropy pair (η, g) for the first-order system (1.4) is an exceptional property since the gradient of g , denoted by $g_{\mathbf{u}}$ and which we assume to be a column vector, the gradient of the entropy function, $\eta_{\mathbf{u}}$, and the Jacobian of \mathbf{f} , denoted by $\mathbf{f}_{\mathbf{u}}$, must satisfy the compatibility condition

$$g_{\mathbf{u}}^T = \eta_{\mathbf{u}}^T \mathbf{f}_{\mathbf{u}}. \quad (1.5)$$

Such an entropy pair exists, however, in the exceptional case $\mathbf{f}_{\mathbf{u}}$ is symmetrizable. In fact, the existence of an entropy pair and the computation of an entropy-conservative flux is a general limitation for the application of entropy-stable methods in the context of systems of conservation laws. Nevertheless, there are many real real-world models for which entropy pairs and entropy conservative numerical fluxes are available, including Euler and related systems, shallow water and related systems, and some multiphase fluid models (see, e.g., [4–8]). In fact, an application to the SW model was considered in [1].

As was derived in [1], the specific limitation in the case of problems with a diffusion term is the additional requirement of positive definiteness of the matrix in entropy variables. Thus, the class of convection-diffusion problems to which the scheme developed in [1] can actually be applied, seems fairly narrow, but it does include a class of diffusively corrected applicative kinematic flow models [9–11], for instance of vehicular traffic or of polydisperse sedimentation. These models can be expressed by (1.1) on a bounded interval I with an arbitrarily large number N of species. It is therefore the purpose of this paper to demonstrate that the entropy stable schemes of [1] can successfully be applied to these models, under modifications due to the presence of boundary conditions but maintaining the principal property of entropy stability.

1.2. Related work. To put this paper further into the proper perspective, we mention that a large number of references to the well-posedness and numerical analysis of (1.1) are provided in [1]. However, the existence and uniqueness of entropy solutions of (1.1), and the convergence of numerical methods have so far only be established in the scalar case ($N = 1$); important contributions in this direction include [12–18] (this list is far from being complete). This state of matters is in agreement with the well-known lack of corresponding results for general first-order systems of conservation laws (1.4) considering that (1.1) reduces to (1.4) wherever $\mathbf{K} = \mathbf{0}$. That said, we mention that

degenerate convection-diffusion systems (1.1) arise in a number of applications such as multiclass vehicular traffic [9–11, 19–21], settling of polydisperse solid-liquid suspensions [10, 11, 22, 23], settling of dispersions of droplets and emulsions [24–26], and chromatography [27, 28]. In particular, in these applications systems of convection-diffusion equations (rather than scalar equations) arise because one wishes to describe the segregation of different classes of units of the disperse phase (cars, particles, droplets, etc.), with the consequence that the number of species N in these applications can be arbitrarily large. These applications motivate the interest in developing efficient solvers for the numerical solution of (1.1), (1.2) or (1.1)–(1.3) even if there is no closed well-posedness theory for these systems. Common numerical schemes are based on a space discretization which can be finite volumes or discontinuous Galerkin methods [29], while the time discretization could be fully explicit or IMEX (see for example [10, 11, 26]). On the explicit side, a well-known scheme is the Kurganov-Tadmor (KT) central scheme, improved later by the related Kurganov-Tadmor high-resolution central difference schemes [30]. The original KT scheme was proposed alongside high-order convex combinations of Runge Kutta time stepping. The latter concept was developed further on, resulting in the so called Strong Stability preserving Runge-Kutta Methods (SSPRK). These schemes allow for a high-order time discretization while preserving the strong stability properties of first-order Euler time stepping, which makes them attractive for solving hyperbolic partial differential equations by the method of lines [31].

1.3. Outline of the paper. The remainder of this paper is organized as follows. In Section 2 we summarize from [1] the construction of entropy stable schemes for (1.1) but extending the discussion to the zero-flux initial-boundary value problem (IBVP) (1.1)–(1.3). Specifically, we discuss in Section 2.1 properties of the continuous problem, and motivate a global entropy inequality for solutions of (1.1)–(1.3). With the goal is to design numerical methods for (1.1), we treat in Section 2.2 the spatial discretization of that equation in the interior of the domain and derive an entropy-conservative numerical flux. The resulting semi-discrete scheme is equipped with a small amount of extra viscosity to prevent oscillations, as is detailed in Section 2.3. Then, in Section 2.4, we outline the numerical scheme that arises from the previous discussion if we wish to solve the zero-flux IBVP (1.1)–(1.3). Results include a time-continuous, spatially discrete entropy inequality. The treatment of Sections 2.2 to 2.4 presupposes that an entropy conservative numerical flux is given, for which we provide in Section 2.5 a sample definition that follows Tadmor [2], and which is utilized in the numerical examples. In Section 3 we outline two applicative models to which the entropy stable schemes are applied, namely in Section 3.1 a diffusively corrected multi-class version of the well-known Lighthill-Whitham-Richards model (DCMCLWR model) that gives rise to the initial value problem (1.1), (1.2), and in Section 3.2 a model of settling of dispersions of droplets and colloidal particles that motivates the IBVP (1.1)–(1.3). Both problems are introduced along with the corresponding entropy conservative numerical flux. Numerical examples for both applicative models are introduced in Section 4, starting with a description of the time discretization and the computation of approximate numerical errors for all cases (in Section 4.1). Examples 1 to 4 (Sections 4.2 to 4.5) deal with the DCMCLWR traffic model, and Examples 5 and 6 (Sections 4.6 and 4.7) are related to the settling model. Conclusions of this study are provided in Section 5.

2. ENTROPY STABLE SCHEMES

2.1. Preliminaries. If there exists a vector-valued function $\mathbb{K} : \Omega \rightarrow \mathbb{R}^N$ such that $\mathbb{K}_{\mathbf{u}} = \mathbf{K}$, where $\mathbb{K}_{\mathbf{u}}$ denotes the Jacobian of the function \mathbb{K} , then the system (1.1) can be written in the form

$$\mathbf{u}_t + \mathbf{f}(\mathbf{u})_x = \mathbb{K}(\mathbf{u})_{xx}.$$

This is always the case for scalar equations if we define

$$\mathbb{K}(u) := \int_0^u \mathbf{K}(\xi) \, d\xi.$$

Let us suppose that the system of conservation laws obtained by dropping the viscous term, i.e., (1.4), is equipped with an entropy pair (η, g) consisting of an entropy function η and an entropy flux g such that $\eta, g : \Omega \rightarrow \mathbb{R}$, η is strictly convex, and (1.5) holds. We then define the so-called entropy variables \mathbf{v} as in [32], namely $\mathbf{v}(\mathbf{u}) := \eta_{\mathbf{u}}(\mathbf{u})$. Then, in order to study the evolution of the entropy for a solution of (1.1), let us first express the diffusion term in terms of the entropy variables. Clearly,

$$(\mathbf{K}(\mathbf{u})\mathbf{u}_x)_x = (\hat{\mathbf{K}}(\mathbf{v})\mathbf{v}_x)_x, \quad (2.1)$$

where we define

$$\hat{\mathbf{K}}(\mathbf{v}) := \mathbf{K}\eta_{\mathbf{u},\mathbf{u}}^{-1}, \quad (2.2)$$

where $\eta_{\mathbf{u},\mathbf{u}}$ is the Hessian matrix of η . The matrix on the left-hand side of (2.1) is evaluated at $\mathbf{u} = \eta_{\mathbf{u}}^{-1}(\mathbf{v})$. Once the diffusion term rewritten, we multiply (1.1) by the vector of entropy variables \mathbf{v} to obtain

$$0 = \mathbf{v}^T \mathbf{u}_t + \mathbf{v}^T \mathbf{f}_{\mathbf{u}}(\mathbf{u})\mathbf{u}_x - \mathbf{v}^T (\hat{\mathbf{K}}(\mathbf{v})\mathbf{v}_x)_x = \eta(\mathbf{u})_t + g(\mathbf{u})_x - (\mathbf{v}^T \hat{\mathbf{K}}(\mathbf{v})\mathbf{v}_x)_x + \mathbf{v}_x^T \hat{\mathbf{K}}(\mathbf{v})\mathbf{v}_x.$$

Therefore, if the matrix $\hat{\mathbf{K}}$ is positive semidefinite, i.e.

$$\mathbf{w}^T \hat{\mathbf{K}}(\mathbf{v})\mathbf{w} \geq 0 \quad \text{for all } \mathbf{w} \in \mathbb{R}^N, \quad (2.3)$$

the following entropy inequality is satisfied:

$$\eta(\mathbf{u})_t + g(\mathbf{u})_x - (\mathbf{v}^T \hat{\mathbf{K}}(\mathbf{v})\mathbf{v}_x)_x \leq 0. \quad (2.4)$$

In the case that $I = \mathbb{R}$ and we consider the initial value problem (1.1), (1.2) under the additional assumption that $\mathbf{u} \rightarrow 0$ when $x \rightarrow \pm\infty$, then the total entropy decreases, i.e.,

$$\frac{d}{dt} \int_{\mathbb{R}} \eta(\mathbf{u}) \, dx \leq 0.$$

(This also includes the case of a finite interval I with solution \mathbf{u} that is compactly supported in I at all times.) On the other hand, considering the IBVP (1.1)–(1.3) and assuming that \mathbf{u} and \mathbf{v} have well defined traces at the boundaries $x = 0$ and $x = L$, which we denote by $\mathbf{u}(0, t)$ and $\mathbf{u}(L, t)$, as well as that the boundary condition (1.3) is well defined in the sense of traces, we can argue as follows. Integrating (2.4) over I , utilizing that $\hat{\mathbf{K}}(\mathbf{v})\mathbf{v}_x = \mathbf{K}(\mathbf{u})\mathbf{u}_x$ and the boundary condition (1.3), we get

$$\begin{aligned} \frac{d}{dt} \int_{\mathbb{R}} \eta(\mathbf{u}) \, dx + g(\mathbf{u}(L, t)) - g(\mathbf{u}(0, t)) &\leq (\mathbf{v}^T \hat{\mathbf{K}}(\mathbf{v})\mathbf{v}_x)|_{x=L} - (\mathbf{v}^T \hat{\mathbf{K}}(\mathbf{v})\mathbf{v}_x)|_{x=0} \\ &= (\mathbf{v}^T \mathbf{K}(\mathbf{u})\mathbf{u}_x)|_{x=L} - (\mathbf{v}^T \mathbf{K}(\mathbf{u})\mathbf{u}_x)|_{x=0} \\ &= \mathbf{v}(L, t)^T \mathbf{f}(\mathbf{u}(L, t)) - \mathbf{v}(0, t)^T \mathbf{f}(\mathbf{u}(0, t)). \end{aligned}$$

In terms of the so-called entropy potential function $\varphi := \mathbf{v}^T \mathbf{f} - g$, we get

$$\frac{d}{dt} \int_{\mathbb{R}} \eta(\mathbf{u}) \, dx \leq \varphi(\mathbf{u}(L, t)) - \varphi(\mathbf{u}(0, t)). \quad (2.5)$$

Note that the function φ , and therefore the right-hand side of (2.5), do not depend on the particular choice of the diffusion matrix $\mathbf{K}(\mathbf{u})$.

Remark 2.1. We emphasize that the requirement that the matrix $\hat{\mathbf{K}}$ defined by (2.2) should be positive semidefinite is the most severe restriction of the applicability of the approach. In fact, for a general positive semidefinite matrix $\mathbf{K} = \mathbf{K}(\mathbf{u})$, the product $\mathbf{K}\eta_{\mathbf{u},\mathbf{u}}^{-1}$ is, in general, not positive semidefinite unless \mathbf{K} and $\eta_{\mathbf{u},\mathbf{u}}^{-1}$ or equivalently, \mathbf{K} and $\eta_{\mathbf{u},\mathbf{u}}$ possess the same set of eigenvectors. That latter property is, however, valid if the diffusion term can be expressed as $\mathbf{K}(\mathbf{u}) = k(\mathbf{u})\mathbf{I}$, where $k(\mathbf{u}) \geq 0$ is a scalar function and \mathbf{I} is the $N \times N$ identity matrix. Then

$$\hat{\mathbf{K}}(\mathbf{v}) = k(\mathbf{u})\eta_{\mathbf{u},\mathbf{u}}^{-1} \quad (2.6)$$

is indeed positive semidefinite, since $\eta_{\mathbf{u},\mathbf{u}}$ is positive definite. Therefore, in this case, (2.4) holds.

2.2. Entropy conservative numerical method. We first consider the case of the initial-value problem (1.1), (1.2) on a standard spatial mesh defined by cells $\mathcal{I}_j := [x_{j-1}, x_j]$, where $x_j = j\Delta x$, $\Delta x = L/M$ for some integer M , and $\mathbf{u}_j(t)$ denotes the cell average of $\mathbf{u}(\cdot, t)$ on \mathcal{I}_j . We will first discretize (1.1) in the interior of the computational domain, and handle the boundary conditions in Section 2.4. To this end, we first consider an entropy-conservative (EC) numerical flux $\mathbf{F}_{j+1/2}$, i.e. a numerical flux satisfying

$$[\mathbf{v}]_{j+1/2}^{\mathbf{T}} \mathbf{F}_{j+1/2} = [\varphi]_{j+1/2}, \quad (2.7)$$

where we employ the following notation to denote the average and jump of any variable ω :

$$[\omega]_{j+1/2} := \omega_{j+1} - \omega_j, \quad \bar{\omega}_{j+1/2} := (\omega_j + \omega_{j+1})/2.$$

Tadmor [2] showed that if the numerical flux $\mathbf{F}_{j+1/2}$ satisfies (2.7), then the solution of the semidiscrete method for (1.4),

$$\mathbf{u}'_j(t) = -\frac{1}{\Delta x}(\mathbf{F}_{j+1/2} - \mathbf{F}_{j-1/2}),$$

where $' \equiv d \cdot / dt$ satisfies the equality

$$\eta(\mathbf{u})'_j(t) = -\frac{1}{\Delta x}(G_{j+1/2} - G_{j-1/2})$$

for some numerical entropy flux $G_{j+1/2}$ consistent with g . Once an EC numerical flux (for (1.4)) has been chosen, we propose the following semidiscrete method for (1.1):

$$\mathbf{u}'_j(t) = -\frac{1}{\Delta x}(\mathbf{F}_{j+1/2} - \mathbf{F}_{j-1/2}) + \frac{1}{\Delta x^2}(\hat{\mathbf{K}}_{j+1/2}[\mathbf{v}]_{j+1/2} - \hat{\mathbf{K}}_{j-1/2}[\mathbf{v}]_{j-1/2}), \quad (2.8)$$

where

$$\hat{\mathbf{K}}_{j+1/2} = \hat{\mathbf{K}}(\bar{\mathbf{v}}_{j+1/2}). \quad (2.9)$$

Let us show that a semidiscrete counterpart of (2.4) is satisfied. Multiplying (2.8) from the left by $\mathbf{v}_j^{\mathbf{T}}$ yields

$$\eta(\mathbf{u})'_j(t) = -\frac{1}{\Delta x}\mathbf{v}_j^{\mathbf{T}}(\mathbf{F}_{j+1/2} - \mathbf{F}_{j-1/2}) + \frac{1}{\Delta x^2}\mathbf{v}_j^{\mathbf{T}}(\hat{\mathbf{K}}_{j+1/2}[\mathbf{v}]_{j+1/2} - \hat{\mathbf{K}}_{j-1/2}[\mathbf{v}]_{j-1/2}).$$

The following identities are obtained by straightforward algebraic manipulations:

$$\begin{aligned} \mathbf{v}_j^{\mathbf{T}} \mathbf{F}_{j+1/2} &= \bar{\mathbf{v}}_{j+1/2}^{\mathbf{T}} \mathbf{F}_{j+1/2} - \frac{1}{2}[\mathbf{v}]_{j+1/2}^{\mathbf{T}} \mathbf{F}_{j+1/2}, \\ \mathbf{v}_j^{\mathbf{T}} \mathbf{F}_{j-1/2} &= \bar{\mathbf{v}}_{j-1/2}^{\mathbf{T}} \mathbf{F}_{j-1/2} + \frac{1}{2}[\mathbf{v}]_{j-1/2}^{\mathbf{T}} \mathbf{F}_{j-1/2}, \\ \mathbf{v}_j^{\mathbf{T}} \hat{\mathbf{K}}_{j+1/2}[\mathbf{v}]_{j+1/2} &= \bar{\mathbf{v}}_{j+1/2}^{\mathbf{T}} \hat{\mathbf{K}}_{j+1/2}[\mathbf{v}]_{j+1/2} - \frac{1}{2}[\mathbf{v}]_{j+1/2}^{\mathbf{T}} \hat{\mathbf{K}}_{j+1/2}[\mathbf{v}]_{j+1/2}, \\ \mathbf{v}_j^{\mathbf{T}} \hat{\mathbf{K}}_{j-1/2}[\mathbf{v}]_{j-1/2} &= \bar{\mathbf{v}}_{j-1/2}^{\mathbf{T}} \hat{\mathbf{K}}_{j-1/2}[\mathbf{v}]_{j-1/2} + \frac{1}{2}[\mathbf{v}]_{j-1/2}^{\mathbf{T}} \hat{\mathbf{K}}_{j-1/2}[\mathbf{v}]_{j-1/2}. \end{aligned} \quad (2.10)$$

From (2.7) we now conclude that

$$\begin{aligned} \mathbf{v}_j^\top (\mathbf{F}_{j+1/2} - \mathbf{F}_{j-1/2}) &= \bar{\mathbf{v}}_{j+1/2}^\top \mathbf{F}_{j+1/2} - \bar{\mathbf{v}}_{j-1/2}^\top \mathbf{F}_{j-1/2} - \frac{1}{2}([\varphi]_{j+1/2} + [\varphi]_{j-1/2}) \\ &= \bar{\mathbf{v}}_{j+1/2}^\top \mathbf{F}_{j+1/2} - \bar{\mathbf{v}}_{j-1/2}^\top \mathbf{F}_{j-1/2} + \bar{g}_{j+1/2} - \bar{g}_{j-1/2} \\ &\quad - \overline{(\mathbf{v}^\top \mathbf{f})}_{j+1/2} + \overline{(\mathbf{v}^\top \mathbf{f})}_{j-1/2}, \end{aligned}$$

while in light of (2.3) we get

$$\mathbf{v}_j^\top (\hat{\mathbf{K}}_{j+1/2}[\mathbf{v}]_{j+1/2} - \hat{\mathbf{K}}_{j-1/2}[\mathbf{v}]_{j-1/2}) \leq \bar{\mathbf{v}}_{j+1/2}^\top \hat{\mathbf{K}}_{j+1/2}[\mathbf{v}]_{j+1/2} - \bar{\mathbf{v}}_{j-1/2}^\top \hat{\mathbf{K}}_{j-1/2}[\mathbf{v}]_{j-1/2}. \quad (2.11)$$

We arrive at the semi-discrete entropy inequality

$$\begin{aligned} \eta(\mathbf{u})'_j(t) + \frac{1}{\Delta x} (G_{j+1/2} - G_{j-1/2}) \\ - \frac{1}{\Delta x^2} (\bar{\mathbf{v}}_{j+1/2}^\top \hat{\mathbf{K}}_{j+1/2}[\mathbf{v}]_{j+1/2} - \bar{\mathbf{v}}_{j-1/2}^\top \hat{\mathbf{K}}_{j-1/2}[\mathbf{v}]_{j-1/2}) \leq 0, \end{aligned} \quad (2.12)$$

where the following numerical entropy flux is obviously consistent with (2.4):

$$G_{j+1/2} = \bar{g}_{j+1/2} + \bar{\mathbf{v}}_{j+1/2}^\top \mathbf{F}_{j+1/2} - \overline{(\mathbf{v}^\top \mathbf{f})}_{j+1/2}. \quad (2.13)$$

2.3. Additional numerical diffusion. In regions where the diffusion matrix \mathbf{K} vanishes, the numerical methods (2.8) or (2.22) reduce to entropy conservative methods whose solutions may exhibit strong oscillations near discontinuities. So to prevent these oscillations some extra numerical diffusion has to be added, either in conservative variables or in entropy variables. Hence the complete scheme is given by

$$\begin{aligned} \mathbf{u}'_j(t) &= -\frac{1}{\Delta x} (\mathbf{F}_{j+1/2} - \mathbf{F}_{j-1/2}) + \frac{1}{\Delta x^2} (\hat{\mathbf{K}}_{j+1/2}[\mathbf{v}]_{j+1/2} - \hat{\mathbf{K}}_{j-1/2}[\mathbf{v}]_{j-1/2}) \\ &\quad + \frac{\varepsilon}{\Delta x^2} ([\mathbf{v}]_{j+1/2} - [\mathbf{v}]_{j-1/2}), \end{aligned} \quad (2.14)$$

where we choose the extra viscosity

$$\varepsilon = \alpha \Delta x \quad (2.15)$$

with a suitable constant $\alpha > 0$.

2.4. Discretization of the initial-boundary value problem with zero-flux boundary conditions. The zero-flux IBVP (1.1)–(1.3) is discretized in space by the following variant of (2.14):

$$\mathbf{u}'_j(t) = -\frac{1}{\Delta x} (\mathbf{J}_{j+1/2} - \mathbf{J}_{j-1/2}), \quad j = 1, \dots, M, \quad (2.16)$$

where we implement (1.3) by setting

$$\mathbf{J}_{j+1/2} = \begin{cases} \mathbf{F}_{j+1/2} - \frac{1}{\Delta x} ((\hat{\mathbf{K}} + \alpha \Delta x \mathbf{I})[\mathbf{v}]_{j+1/2}) & \text{for } j = 1, \dots, M-1, \\ \mathbf{0} & \text{for } j = 0 \text{ and } j = M. \end{cases} \quad (2.17)$$

For the analysis of the entropy inequality let us again suppose that $\alpha = 0$. Then the scheme (2.16), (2.17) satisfies the semi-discrete entropy inequality (2.12) for $j = 2, \dots, M-1$. On the other hand, for $j = 1$ we obtain by calculations similar to (2.10)–(2.11), and utilizing (2.7) for $j = 1$, from

$$\eta(\mathbf{u})'_1(t) + \frac{1}{\Delta x} \mathbf{v}_1^\top \mathbf{F}_{3/2} - \frac{1}{\Delta x^2} \mathbf{v}_1^\top \hat{\mathbf{K}}_{3/2}[\mathbf{v}]_{3/2} = 0$$

the inequality

$$\eta(\mathbf{u})'_1(t) + \frac{1}{\Delta x} \left(\bar{\mathbf{v}}_{3/2}^T \mathbf{F}_{3/2} - \frac{1}{2} [\varphi]_{3/2} \right) - \frac{1}{\Delta x^2} \bar{\mathbf{v}}_{3/2}^T \hat{\mathbf{K}}_{3/2} [\mathbf{v}]_{3/2} \leq 0.$$

A straightforward calculation and taking into account (2.13) for $j = 1$ reveal that

$$\bar{\mathbf{v}}_{3/2}^T \mathbf{F}_{3/2} - \frac{1}{2} [\varphi]_{3/2} = G_{3/2} - g_1 + \mathbf{v}_1^T \mathbf{f}_1 = G_{3/2} + \varphi(\mathbf{u}_1(t)),$$

hence we obtain

$$\eta(\mathbf{u})'_1(t) + \frac{1}{\Delta x} (G_{3/2} + \varphi(\mathbf{u}_1(t))) - \frac{1}{\Delta x^2} \bar{\mathbf{v}}_{3/2}^T \hat{\mathbf{K}}_{3/2} [\mathbf{v}]_{3/2} \leq 0. \quad (2.18)$$

For $j = M$ we deduce by analogous arguments from

$$\eta(\mathbf{u})'_M(t) - \frac{1}{\Delta x} \mathbf{v}_M^T \mathbf{F}_{M-1/2} + \frac{1}{\Delta x^2} \mathbf{v}_M^T \hat{\mathbf{K}}_{M-1/2} [\mathbf{v}]_{M-1/2} = 0$$

the inequality

$$\eta(\mathbf{u})'_M(t) - \frac{1}{\Delta x} (G_{M-1/2} + \varphi(\mathbf{u}_M(t))) + \frac{1}{\Delta x^2} \bar{\mathbf{v}}_{M-1/2}^T \hat{\mathbf{K}}_{M-1/2} [\mathbf{v}]_{M-1/2} \leq 0. \quad (2.19)$$

Let us now define

$$\eta(\mathbf{u})'_{\text{tot}}(t) := \Delta x \sum_{j=1}^M \eta(\mathbf{u})'_j(t).$$

Then, summing (2.18), (2.12) for $j = 2, \dots, M-1$, and (2.19), and multiplying the result by Δx , we obtain the inequality

$$\eta(\mathbf{u})'_{\text{tot}}(t) \leq \varphi(\mathbf{u}_M(t)) - \varphi(\mathbf{u}_1(t)), \quad (2.20)$$

which is a discrete analogue of (2.5).

2.5. Construction of an entropy conservative (EC) numerical flux. Following Tadmor [2], we may obtain an entropy conservative (EC) numerical flux by solving the following integral:

$$\mathbf{F}_{j+1/2} = \int_0^1 \mathbf{f}(\mathbf{u}(\mathbf{w}_j + s(\mathbf{w}_{j+1} - \mathbf{w}_j))) \, ds. \quad (2.21)$$

Remark 2.2. *An alternative way of constructing entropy stable schemes could be the following. Suppose that, given \mathbf{u}_L and \mathbf{u}_R , there exists an approximation of $\boldsymbol{\eta}_{\mathbf{u}, \mathbf{u}}$, denoted by $\mathbf{H}(\mathbf{u}_L, \mathbf{u}_R)$, that satisfies the Roe-like property $\mathbf{v}_R - \mathbf{v}_L = \mathbf{H}(\mathbf{u}_L, \mathbf{u}_R)(\mathbf{u}_R - \mathbf{u}_L)$. We may then consider the numerical method*

$$\mathbf{u}'_j(t) = -\frac{1}{\Delta x} (\mathbf{F}_{j+1/2} - \mathbf{F}_{j-1/2}) + \frac{1}{\Delta x^2} (\hat{\mathbf{K}}_{j+1/2} [\mathbf{u}]_{j+1/2} - \hat{\mathbf{K}}_{j-1/2} [\mathbf{u}]_{j-1/2}), \quad (2.22)$$

where $\mathbf{K}_{j+1/2} = \hat{\mathbf{K}}_{j+1/2} \mathbf{H}_{j+1/2}$. Here, $\hat{\mathbf{K}}_{j+1/2}$ is given by (2.9) and $\mathbf{H}_{j+1/2} = \mathbf{H}(\mathbf{u}_j, \mathbf{u}_{j+1})$. The equality

$$\mathbf{K}_{j+1/2} [\mathbf{u}]_{j+1/2} = \hat{\mathbf{K}}_{j+1/2} [\mathbf{v}]_{j+1/2}$$

allows one to prove the entropy inequality (2.12) reasoning as in the previous case.

3. APPLICATIVE MODELS

3.1. A diffusively corrected multi-class traffic model (DCMCLWR model). We consider the system (1.1) with a flux function defined by

$$\mathbf{f}(\mathbf{u}) = V(u)(v_1^{\max}u_1, \dots, v_N^{\max}u_N)^{\mathsf{T}}, \quad (3.1)$$

where v_i^{\max} is the preferential (maximum) velocity of species i (driver class i); $u = u_1 + \dots + u_N$ is the total density; and V is a hindrance function that is usually assumed to satisfy

$$V(0) = 1, \quad V(u_{\max}) = 0, \quad V'(u) < 0 \quad \text{for } 0 < u < u_{\max},$$

where u_{\max} is a maximum density. We assume, furthermore, that $v_1^{\max} > v_2^{\max} > \dots > v_N^{\max}$. Under these assumptions on \mathbf{f} , the first-order system (1.4) corresponds to the multiclass extension, introduced in [19, 33], of the well-known Lighthill-Whitham-Richards (LWR) single-class kinematic traffic model [34, 35]. An entropy pair (η, g) for this multiclass model is given by [20]

$$\eta(\mathbf{u}) = \sum_{i=1}^N \frac{u_i(\log(u_i) - 1)}{v_i^{\max}}, \quad g(\mathbf{u}) = V(u) \sum_{i=1}^N u_i \log(u_i) - \mathcal{V}(u), \quad (3.2)$$

where $\mathcal{V}(u)$ is any primitive of $V(u)$. Using $\mathbf{v}(\mathbf{u}) := \eta_{\mathbf{u}}(\mathbf{u})$ (see Section 2.1) we then obtain the entropy variables $\mathbf{w} = (w_1, \dots, w_N)^{\mathsf{T}}$ given by

$$w_i = \frac{\log(u_i)}{v_i^{\max}} \Leftrightarrow u_i = \exp(w_i v_i^{\max}), \quad i = 1, \dots, N.$$

In addition, the following notation will be used:

$$\mathbf{w} := \sum_{i=1}^N \exp(v_i^{\max} w_i).$$

Notice that the transformation $\mathbf{u} \rightarrow \mathbf{w}$ is one-to-one from $(0, \infty)^N$ to \mathbb{R}^N , but is not defined when $u_i = 0$.

Now we associate the behavior of drivers with an anticipation distance L_{\min} . Then the reaction of a driver depends on the function $p_i(x, t) := u(x + L_{\min}, t)$. Using a Taylor expansion of $V(p_i(x, t))$ around $u(x, t)$, we obtain

$$V(p_i(x, t)) = V(u) + V'(u)(L_{\min} \partial_x u) + \mathcal{O}(L_{\min}^2).$$

Neglecting the $\mathcal{O}(L_{\min}^2)$ term and inserting the remaining expression into (1.1), we have

$$\partial_t u_i(x, t) + \partial_x (u_i(x, t) v_i^{\max} V(u)) = \partial_x (-L_{\min} V'(u) u_i(x, t) v_i^{\max} \partial_x u(x, t)).$$

To further simplify the model we remove the dependencies on individual driver classes. Hence, we propose to use the semipositive definite diffusion matrix

$$\mathbf{K}(\mathbf{u}) = \beta(u) \mathbf{I}, \quad (3.3)$$

where \mathbf{I} denotes the $N \times N$ identity matrix and $\beta(u) \geq 0$ is a scalar function. Since we prefer to work in entropy variables, following (2.6), the diffusion matrix is defined as

$$\hat{\mathbf{K}}(\mathbf{v}) = \mathbf{K}(\mathbf{u}) \eta_{\mathbf{u}, \mathbf{u}}(\mathbf{u})^{-1} = \beta(w) \text{diag}(v_1^{\max} \exp(v_1^{\max} w_1), \dots, v_N^{\max} \exp(v_N^{\max} w_N)). \quad (3.4)$$

For this example we will use the hindrance function $V(u) = 1 - u$ due to Greenshields [36]. Replacing this function in (3.1) and solving (2.21), we get the entropy stable numerical flux

$$\mathbf{F}_{j+1/2} = (F_{1,j+1/2}, \dots, F_{N,j+1/2})^{\mathsf{T}}, \quad (3.5)$$

where

$$F_{i,j+1/2} = v_i^{\max} \left(\frac{u_{j+1,i} - u_{j,i}}{\log(u_{j+1,i}) - \log(u_{j,i})} - \sum_{k=1}^N \frac{u_{j+1,k}u_{j+1,i} - u_{j,k}u_{j,i}}{\log(u_{j+1,k}u_{j+1,i}) - \log(u_{j,k}u_{j,i})} \right), \quad i = 1, \dots, N. \quad (3.6)$$

Equations (3.4)–(3.6) complete the definition of the semi-discrete numerical scheme (2.14).

Remark 3.1. *In order to get rid of the singularity of the entropy variables when one of the terms in the log differences in (3.6) is zero or the difference is zero, we use the following third-order approach:*

$$\log(u) - \log(v) \approx \frac{u - v}{0.5(u + v)}.$$

An alternative stable numerical algorithm used to compute the logarithmic mean when $u \approx v$ is given in [37, App. B] and will be used in the second application problem.

Remark 3.2. *Although we considered other forms for the hindrance function, the integral (2.21) it is difficult to compute in general or can result in a numerically unstable flux [30]. Indeed equation (2.21) results in a closed form only for a limited selection of functions, such as functions of the form $V(u) = (1 - u)^n$ with n an integer. We are aware that the development of entropy stable flows for more general forms of flow functions in multispecies kinematic flow models needs more extensive study.*

3.2. Settling of dispersions of droplets and colloidal particles. The settling of a dispersion of droplets or that of a suspension of colloidal solid particles dispersed in a fluid can be modeled by system of convection-diffusion equations of the form (1.1) for $I = [0, L]$, where t is time, x is depth, and $\mathbf{u}(x, t)$ is the vector of volume fractions of particles u_i of class i , $i = 1, \dots, N$ [26]. The problem (1.1), (1.2) is completed with the zero-flux boundary condition (1.3).

Particles are characterized by their diameter d_i and settling velocities $v_1 > v_2 > \dots > v_N$. Moreover, we assume that the flux vector $\mathbf{f}(\mathbf{u})$ has the form

$$\mathbf{f}(\mathbf{u}) = V(u)(v_1 u_1, \dots, v_N u_N)^T,$$

where again $u := u_1 + \dots + u_N$. According to [25], the Stokes terminal velocities v_i are given by

$$v_i = \frac{(\rho_d - \rho_c)g d_i^2}{18\mu_c}, \quad i = 1, \dots, N,$$

where ρ and μ , respectively, denote density and viscosity, and the indices d and c respectively, refer to the disperse or continuous phase, and in this formula $g = 9.81 \text{ m/s}^2$ is the acceleration of gravity. A common choice for the so-called hindered settling function $V(u)$ is given by Richardson-Zaki [38] expression:

$$V(u) = \begin{cases} (1 - u)^{n_{\text{RZ}}} & \text{if } u \leq 1, \\ 0 & \text{if } u > 1. \end{cases} \quad (3.7)$$

The diffusion matrix is again defined by (3.3), where $\beta(u) = D_0 V(u)$ for some constant $D_0 > 0$. For the numerical examples we choose $n_{\text{RZ}} = 2$, following the same procedure as in the previous application, the numerical diffusion is given by (3.4) and the numerical flux function, obtained from

(2.21), is now given by (3.5) with

$$\begin{aligned}
F_{i,j+1/2}^n = v_i^{\max} & \left(\frac{u_{j+1,i} - u_{j,i}}{\log(u_{j+1,i}) - \log(u_{j,i})} - 2 \sum_{k=1}^N \frac{u_{j+1,k} u_{j+1,i} - u_{j,k} u_{j,i}}{\log(u_{j+1,k} u_{j+1,i}) - \log(u_{j,k} u_{j,i})} \right. \\
& + \sum_{k=1}^N \frac{u_{j+1,k}^2 u_{j+1,i} - u_{j,k}^2 u_{j,i}}{\log(u_{j+1,k}^2 u_{j+1,i}) - \log(u_{j,k}^2 u_{j,i})} \\
& \left. + \sum_{\substack{k,l=1 \\ k \neq l}}^N \frac{u_{j+1,k} u_{j+1,l} u_{j+1,i} - u_{j,k} u_{j,l} u_{j,i}}{\log(u_{j+1,k} u_{j+1,l} u_{j+1,i}) - \log(u_{j,k} u_{j,l} u_{j,i})} \right), \quad i = 1, \dots, N.
\end{aligned} \tag{3.8}$$

For the computation of the logarithmic mean we use the numerically stable procedure described by Ismail and Roe [37, Appendix B].

4. NUMERICAL EXAMPLES

4.1. Preliminaries. For the time integration in all examples, we use a second-order strong stability preserving Runge-Kutta scheme (SSPRK2 or also known as Heun's method), i.e. for a given a spatial discretization $\mathbf{h}(\mathbf{u})$, the integration scheme for the system $\mathbf{u}'(t) = \mathbf{h}(\mathbf{u})$ is given as follows, where we assume that we wish to advance the solution from $\mathbf{u}^n \approx \mathbf{u}(t_n)$ to $\mathbf{u}^{n+1} \approx \mathbf{u}(t_{n+1})$, where $t_{n+1} = t_n + \Delta t$:

$$\begin{aligned}
\mathbf{u}^{(1)} &= \mathbf{u}^n + \Delta t \mathbf{h}(\mathbf{u}^n), \\
\mathbf{u}^{(2)} &= \mathbf{u}^{(1)} + \Delta t \mathbf{h}(\mathbf{u}^{(1)}), \\
\mathbf{u}^{n+1} &= \frac{1}{2}(\mathbf{u}^n + \mathbf{u}^{(2)}), \quad n = 0, 1, 2, \dots
\end{aligned}$$

We choose the time step Δt at each iteration t_n according to the following CFL condition:

$$\frac{\Delta t}{\Delta x} \max_{1 \leq j \leq M} \rho(\mathbf{f}_u(\mathbf{u}_j^n)) + \frac{\Delta t}{2\Delta x^2} \max_{1 \leq j \leq M} \rho(\mathbf{K}(\mathbf{u}_j^n)) = C_{\text{CFL}} \tag{4.1}$$

where $\rho(\cdot)$ is the spectral radius. In all cases, we calculate the approximate total L^1 error at a given time t as follows. We assume that the spatial computational domain is subdivided into M equal-sized cells of width Δx , and that we calculate approximate errors by utilizing a reference solution defined on a mesh with $M_{\text{ref}} > M$ cells, where we assume that $R := M_{\text{ref}}/M$ is an integer. Then we calculate the projection of the reference solution onto the coarser grid,

$$\tilde{u}_{j,i}^{\text{ref}}(t) = \frac{1}{R} \sum_{k=1}^R u_{R(j-1)+k,i}^{\text{ref}}(t), \quad j = 1, \dots, M, \quad i = 1, \dots, N, \tag{4.2}$$

and then calculate the total approximate total L^1 error by summing the corresponding errors of each species, that is,

$$e_M^{\text{tot}} = \frac{1}{M} \sum_{i=1}^N \sum_{j=1}^M |\tilde{u}_{j,i}^{\text{ref}}(t) - u_{j,i}^M(t)|. \tag{4.3}$$

The corresponding (approximate) convergence rate between successive grids with discretizations $M/2$ and M is given by

$$\theta_M := \log_2(e_{M/2}^{\text{tot}}/e_M^{\text{tot}}). \tag{4.4}$$

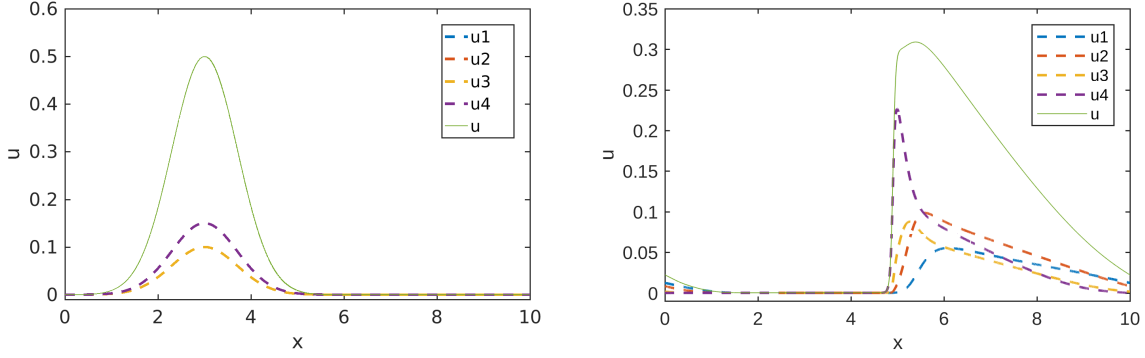


FIGURE 1. Example 1 (traffic model, non-degenerate diffusion, $N = 4$): (left) initial condition (4.6), (right) reference numerical solution at simulated time $t = 0.1$ h obtained by the EC scheme with $\alpha = 1.5$ and $M_{\text{ref}} = 12800$.

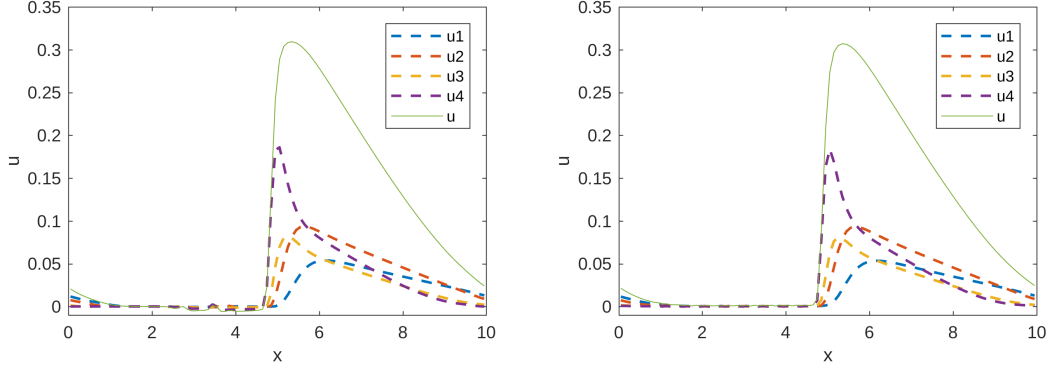


FIGURE 2. Example 1 (traffic model, non-degenerate diffusion, $N = 4$): numerical solution at simulated time $t = 0.1$ h obtained by the entropy stable scheme with $M = 100$ and (left) with zero extra viscosity, (right) with extra viscosity (2.15) with $\alpha = 1.5$.

4.2. Example 1 (traffic model, non-degenerate diffusion, $N = 4$). First, we test the entropy conserving scheme on a regular grid. We consider a circular road of length $L = 10$ mi and $N = 4$ driver classes with the velocities $v_1^{\max} = 60$ mi/h, $v_2^{\max} = 55$ mi/h, $v_3^{\max} = 50$ mi/h, and $v_4^{\max} = 45$ mi/h, along with a uniform anticipation length of $L_{\min} = 0.03$ mi and the non-degenerate diffusion term defined by (3.3) and

$$\beta(u) = \frac{L_{\min}}{N} (\overline{v^{\max}}), \quad \overline{v^{\max}} := \frac{1}{N} \sum_{i=1}^N v_i^{\max}. \quad (4.5)$$

The initial traffic platoon (see Figure 1 (left)) is given by

$$\mathbf{u}_0(x, 0) = p(x)(0.2, 0.3, 0.2, 0.3)^T, \quad p(x) = 0.5 \exp(-(x - 3)^2). \quad (4.6)$$

Numerical approximations are computed with $C_{\text{CFL}} = 0.25$ at simulated time $t = 0.1$ h using the method of lines of the semidiscretization given by the numerical flux (3.6), and the numerical diffusion (3.4). The performances of the entropy stable (EC) scheme without and with extra

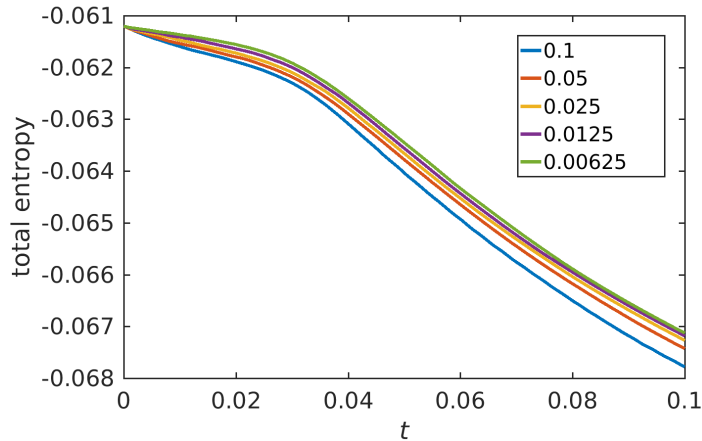


FIGURE 3. Example 1 (traffic model, non-degenerate diffusion, $N = 4$): total entropy $\mathcal{E}_n^{\text{tot}}$ of the numerical solution at different mesh sizes, based on the extra viscosity (2.15) with $\alpha = 1.5$.

M	KT		LLF		EC ($\alpha = 1.5$)	
	e_M^{tot}	θ_M	e_M^{tot}	θ_M	e_M^{tot}	θ_M
100	4.024e-2	—	1.445e-1	—	3.140e-2	—
200	1.524e-2	1.401	8.830e-2	0.711	1.379e-2	1.188
400	5.881e-3	1.374	5.119e-2	0.786	6.857e-3	1.008
800	4.232e-3	0.475	2.868e-2	0.836	3.212e-3	1.094
1600	3.637e-4	0.219	1.574e-2	0.866	1.369e-3	1.230
3200	3.350e-4	0.055	8.718e-3	0.853	5.476e-4	1.322

TABLE 1. Example 1 (traffic model, non-degenerate diffusion, $N = 4$): approximate total L^1 errors (e_M^{tot}) and convergence rates (θ_M) at simulated time $t = 0.1$.

viscosity are compared in Figure 2. Here and in Examples 2 to 4 we also verify that the method is indeed entropy stable by plotting the following total entropy for $t = t_n = n\Delta t$:

$$\mathcal{E}_n^{\text{tot}} := \sum_{j=1}^M \overline{\eta(\mathbf{u}_j(t_n))} \Delta x,$$

see Figure 3 for this example. We observe that this quantity decreases in time at all discretizations, as expected. Moreover, in this example the approximate total L^1 errors were computed by using a numerical reference solution (EC scheme with $M_{\text{ref}} = 12800$, $\alpha = 1.5$), and are shown in Table 1. For comparison solutions obtained with Kurganov-Tadmor (KT) scheme and local Lax-Friedrichs (LLF) scheme, augmented by (3.4) are also presented. With respect to the error table, we observe that the EC scheme exhibits convergence rates that are consistently slightly large than one. The smallness of the error observed for $M = 3200$ has to be interpreted carefully due to the proximity to the reference solution.

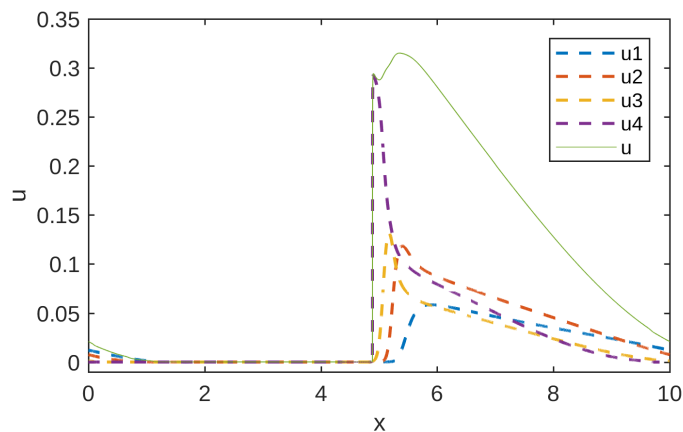


FIGURE 4. Example 2 (traffic model, continuous degenerate diffusion, $N = 4$): reference numerical solution at simulated time $t = 0.1$ h obtained by the EC scheme with $\alpha = 1.5$ and $M_{\text{ref}} = 12800$.

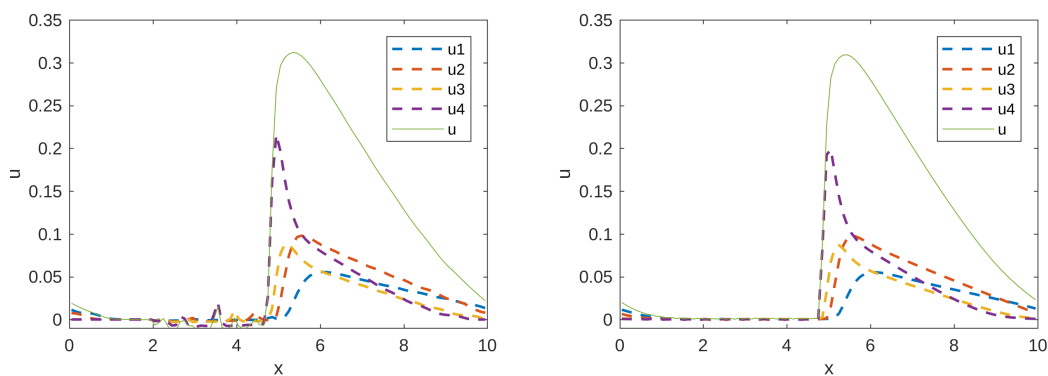


FIGURE 5. Example 2 (traffic model, continuous degenerate diffusion, $N = 4$): numerical solution at simulated time $t = 0.1$ h obtained by the entropy stable scheme with $M = 100$ and (left) with zero extra viscosity, (right) with extra viscosity (2.15) with $\alpha = 1.5$.

4.3. Example 2 (traffic model, continuous degenerate diffusion, $N = 4$). In Example 2, under the same initial conditions as in Example 1, we test the model with the diffusion matrix (3.3), where we define

$$\beta(u) = \begin{cases} 0 & \text{if } u \leq u_c, \\ \frac{L_{\min} v^{\max}}{N} (u - u_c) & \text{if } u > u_c, \end{cases}$$

where $\overline{v^{\max}}$ is defined as in (4.5), and we choose $u_c = 0.2$. The new diffusion matrix now depends on the total density $u = u_1 + \dots + u_N$ and vanishes when $u \leq u_c$, but is still a continuous function of u . Note that since $\beta(u) = 0$ for $u \leq u_c$, for these u -values the method (2.8) is reduced to an entropy conservative method for first-order systems of conservation laws that exhibits oscillations. The resulting model is strongly degenerate and requires more extra viscosity. Figure 6 confirms that also this example exhibits a decrease in approximate total entropy. Approximate L^1 -errors

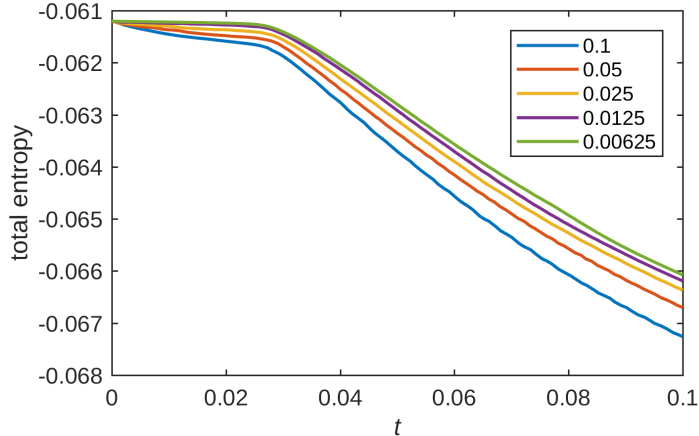


FIGURE 6. Example 2 (traffic model, continuous degenerate diffusion, $N = 4$): total entropy $\mathcal{E}_n^{\text{tot}}$ of the numerical solution at different mesh sizes, based on the extra viscosity (2.15) with $\alpha = 1.5$.

M	KT			LLF			EC ($\alpha = 1.5$)		
	e_M^{tot}	θ_M	cpu[s]	e_M^{tot}	θ_M	cpu[s]	e_M^{tot}	θ_M	cpu[s]
100	7.846e-2	—	0.76	1.722e-1	—	0.52	6.108e-2	—	0.36
200	4.327e-2	0.859	3.00	1.166e-1	0.562	2.09	3.254e-2	0.908	1.41
400	1.749e-2	1.306	11.50	8.042e-2	0.537	8.19	1.5425e-2	1.078	5.56
800	7.710e-3	1.182	46.51	5.284e-2	0.606	32.82	9.020e-3	0.773	22.23
1600	4.011e-3	0.943	197.69	3.225e-2	0.712	134.94	5.433e-3	0.731	91.72
3200	2.707e-3	0.567	863.22	1.884e-2	0.775	626.73	2.466e-3	1.139	413.56

TABLE 2. Example 2 (traffic model, continuous degenerate diffusion, $N = 4$): approximate L^1 errors (e_M^{tot}), convergence rates (θ_M), and cpu times (cpu) at simulated time $t = 0.1$.

for u computed by a numerical reference solution (EC scheme with $M_{\text{ref}} = 12800$, $\alpha=1.5$) are shown in Table 2. That table also shows CPU times. It is worth noting that the EC scheme is the one that executes most rapidly and produces errors that are only slightly larger in some instances than those of the KT scheme at the same discretization. Thus, we can say that the EC scheme is the most efficient (in terms of error reduction versus CPU time) in this case.

4.4. Example 3 (traffic model, discontinuous degenerate diffusion, $N = 4$). Under the same initial conditions of Examples 1 and 3, now we test the model with the diffusion matrix (3.3) with

$$\beta(u) = \begin{cases} 0 & \text{if } u \leq u_c, \\ L_{\min} \overline{v^{\max}} / N & \text{if } u > u_c, \end{cases}$$

where $\overline{v^{\max}}$ is still defined as in (4.5) and we choose $u_c = 0.2$. Note that the resulting model is strongly degenerate and requires more extra viscosity as in Example 2, but that an additional complication comes from the fact that β , and therefore \mathbf{K} , are now a discontinuous function

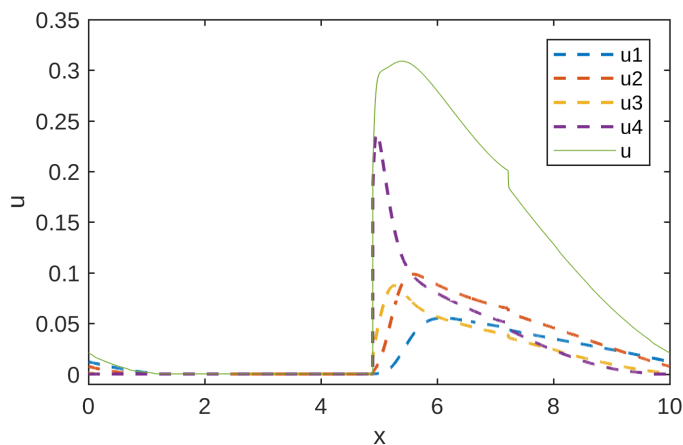


FIGURE 7. Example 3 (traffic model, discontinuously degenerate diffusion, $N = 4$): reference numerical solution at simulated time $t = 0.1$ h obtained by the EC scheme with $\alpha = 1.5$ and $M_{\text{ref}} = 12800$.

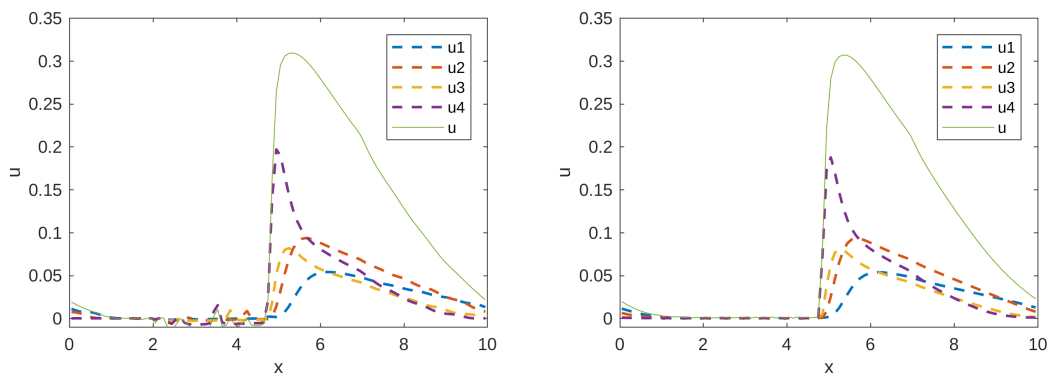


FIGURE 8. Example 3 (traffic model, discontinuous degenerate diffusion, $N = 4$): numerical solution at simulated time $t = 0.1$ h obtained by the entropy stable scheme with $M = 100$ and (left) with zero extra viscosity, (right) with extra viscosity (2.15) with $\alpha = 1.5$.

of u . Figure 7 shows the reference solution obtained for this case, and Figure 8 displays numerical solutions with $M = 100$. Entropy stability still holds, as depicted in Figure 9. The approximate L^1 -errors for u computed by using a numerical reference solution (EC scheme with $M_{\text{ref}} = 12800$, $\alpha = 1.5$) are shown in Table 3.

4.5. Example 4 (traffic model, continuous degenerate diffusion, non-smooth initial datum, $N = 4$). Under the assumptions of Example 2, we replace the smooth initial condition (4.6)

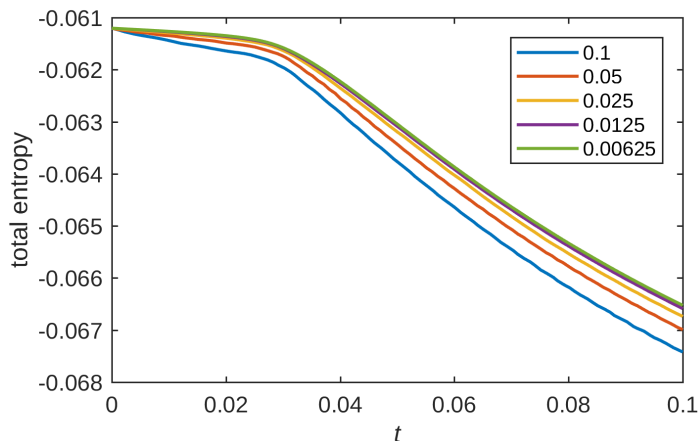


FIGURE 9. Example 3 (traffic model, discontinuous degenerate diffusion, $N = 4$): total entropy $\mathcal{E}_n^{\text{tot}}$ of the numerical solution at different mesh sizes, based on the extra viscosity (2.15) with $\alpha = 1.5$.

M	KT			LLF			EC ($\alpha = 1.5$)		
	e_M^{tot}	θ_M	cpu[s]	e_M^{tot}	θ_M	cpu[s]	e_M^{tot}	θ_M	cpu[s]
100	4.742e-2	—	0.78	1.486e-1	—	0.53	3.796e-2	—	0.37
200	2.053e-2	1.207	2.97	9.143e-2	0.701	2.26	1.814e-2	1.065	1.41
400	9.797e-3	1.069	12.83	5.348e-2	0.774	8.92	9.037e-3	1.005	6.06
800	6.752e-3	0.535	55.48	3.130e-2	0.773	38.36	4.301e-3	1.071	26.06
1600	4.941e-3	0.450	350.13	1.793e-2	0.804	168.91	2.102e-3	1.033	233.55
3200	4.536e-3	0.123	1452.28	1.043e-2	0.781	984.89	1.333e-3	0.656	656.21

TABLE 3. Example 3 (traffic model, continuous degenerate diffusion, $N = 4$): approximate L^1 errors (e_M^{tot}), convergence rates (θ_M), and cpu times (cpu) at simulated time $t = 0.1$.

M	KT			EC ($\alpha = 1.5$)			CU		
	e_M^{tot}	θ_M	cpu[s]	e_M^{tot}	θ_M	cpu[s]	e_M^{tot}	θ_M	cpu[s]
100	1.365e-1	—	1.92	32.053*	—	97.43	1.216e-1	—	1.78
200	7.765e-2	0.814	3.34	7.408e-2	—	2.22	6.948e-2	0.807	4.49
400	3.751e-2	1.050	14.67	3.931e-2	0.914	10.09	3.417e-2	1.024	20.34
800	1.843e-2	1.025	59.91	2.157e-2	0.866	42.54	1.707e-2	1.001	81.32
1600	1.030e-3	0.840	219.62	1.142e-2	0.918	151.49	9.736e-3	0.811	298.57
3200	8.006e-3	0.363	963.64	6.921e-3	0.722	785.65	8.562e-3	0.185	1362.84

TABLE 4. Example 4 (traffic model, continuous degenerate diffusion, non-smooth initial datum, $N = 4$): approximate L^1 errors (e_M^{tot}), convergence rates (θ_M), and cpu times (cpu) at simulated time $t = 0.2$.

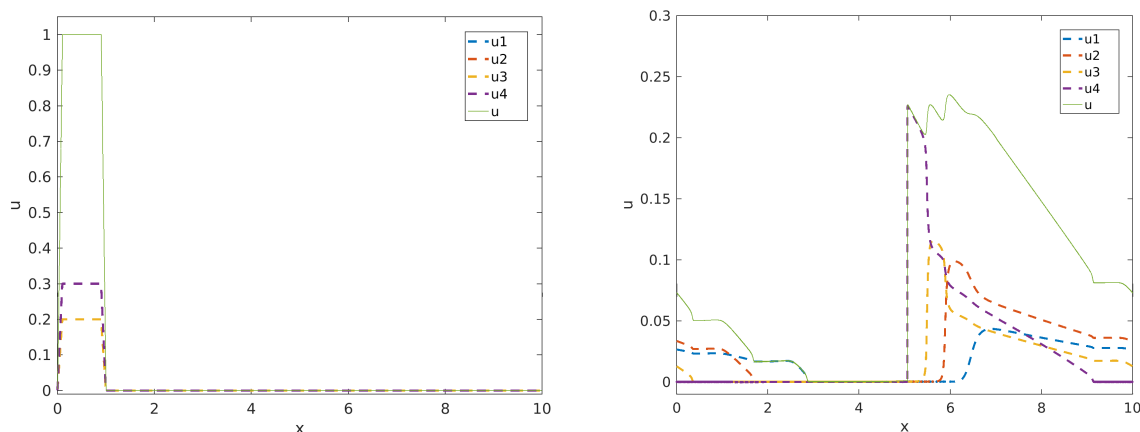


FIGURE 10. Example 4 (traffic model, continuous degenerate diffusion, non-smooth initial datum, $N = 4$): (left) initial condition (4.7), (right) reference numerical solution at simulated time $t = 0.1$ h obtained by the EC scheme with $\alpha = 1.5$ and $M_{\text{ref}} = 12800$.

	i	1	2	3	4	5	6	7	8
20% glycerol	$d_i[\mu\text{m}]$	201.430	140.2	99.751	68.986	48.391	34.185	23.810	6.101
	$\phi_i^0[\%]$	0.0859	0.6410	4.4309	7.928	4.7065	1.5710	0.5720	0.1758
50% glycerol	$d_i[\mu\text{m}]$	417.819	291.590	202.854	143.384	100.118	68.629	48.259	33.886
	$\phi_i^0[\%]$	0.329	11.380	25.010	9.921	2.305	0.821	0.502	0.183

TABLE 5. Example 5 and 6 (settling model, discontinuous degenerate diffusion, $N = 8$): droplet particle diameters d_i and initial concentrations ϕ_i^0 .

by the following function, corresponding to a “platoon” of traffic:

$$\mathbf{u}_0(x, 0) = p(x)(0.2, 0.3, 0.2, 0.3)^T, \quad p(x) = \begin{cases} 10x & \text{for } 0 < x \leq 0.1, \\ 1 & \text{for } 0.1 < x \leq 0.9, \\ -10(x - 1) & \text{for } 0.9 < x \leq 1, \\ 0 & \text{otherwise.} \end{cases} \quad (4.7)$$

As is shown in Figure 11 (top), this set of initial conditions causes strong oscillations near the transition between hyperbolic and parabolic regimes. On the $M = 100$ mesh, these oscillations produce artifacts that remain through time iterations even with high extra viscosity. In order to avoid these artifacts, a finer mesh was required; Figure 11 (bottom) compares the entropy conservative scheme solution against a solution by the KT scheme with $M = 800$. In Table 4 we show L^1 -errors for u computed by a numerical reference solution (EC scheme with $\alpha = 1.5$, $M_{\text{ref}} = 12800$). The large value of the $M = 100$ entry for the EC scheme in that table indicates that additional numerical viscosity was not sufficient to prevent strong oscillations (see Figure 11). A numerical solution obtained with the less diffusive central-upwind (CU) scheme by Kurganov et al. [39] is also presented for comparison.

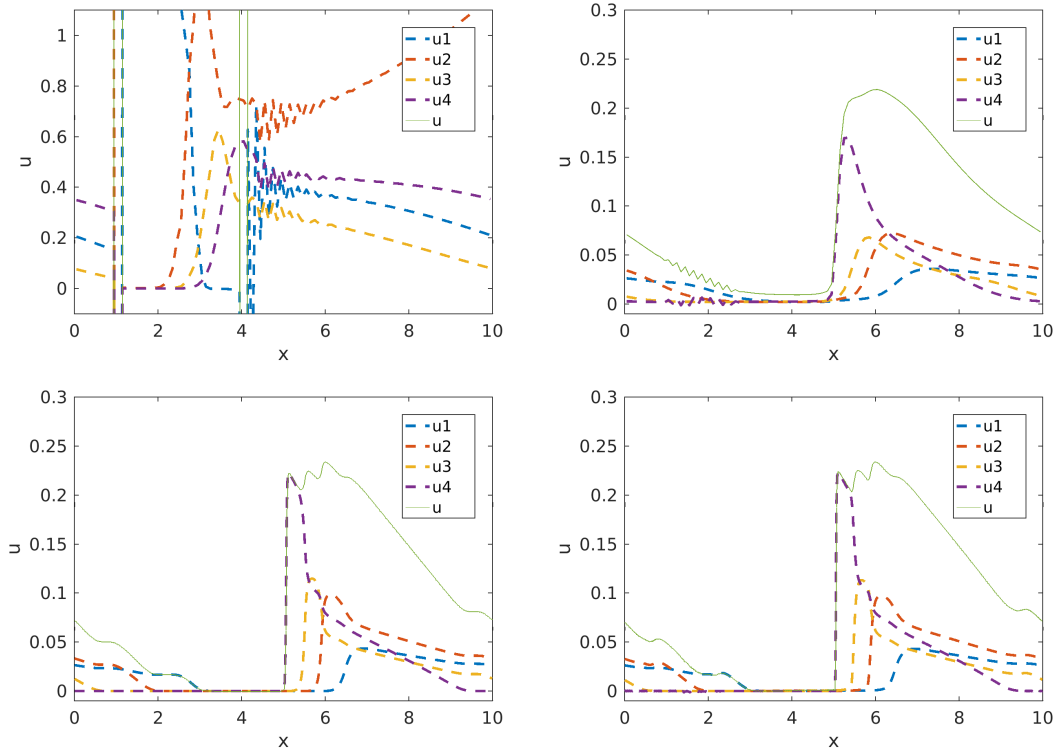


FIGURE 11. Example 4 (traffic model, continuous degenerate diffusion, non-smooth initial datum, $N = 4$): numerical solution at simulated time $t = 0.2$ h (top) obtained by the entropy stable scheme with $M = 100$ and (left) with zero extra viscosity, (right) with extra viscosity (2.15) with $\alpha = 8$, (bottom) with $M = 800$ and (left) with the KT scheme, (right) with the entropy stable scheme with extra viscosity (2.15) with $\alpha = 1.5$.

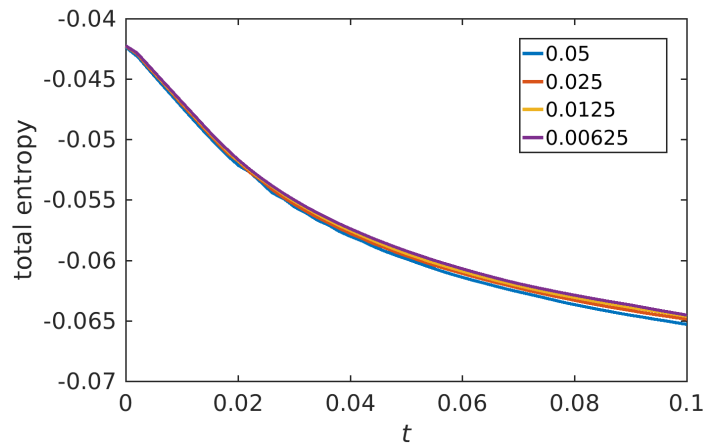


FIGURE 12. Example 4 (traffic model, continuous degenerate diffusion, non-smooth initial datum, $N = 4$): total entropy $\mathcal{E}_n^{\text{tot}}$ of the numerical solution of the EC scheme (extra viscosity (2.15) with $\alpha = 1.5$) at different mesh sizes.

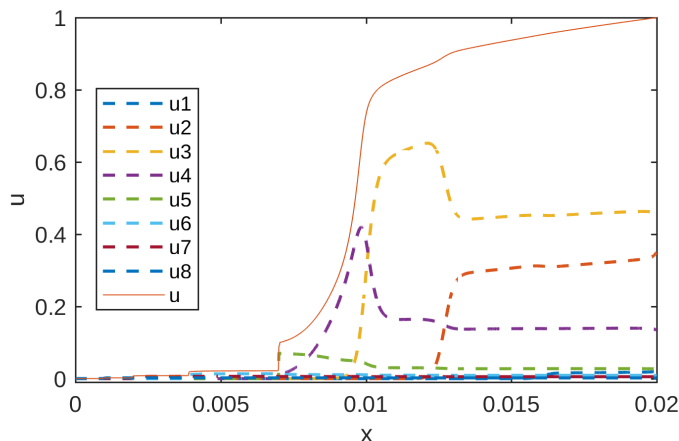


FIGURE 13. Example 5 (settling model, discontinuous degenerate diffusion, $N = 8$): reference solution at simulated time $t = 50$ calculated by the GLF scheme with $M_{\text{ref}} = 6400$.

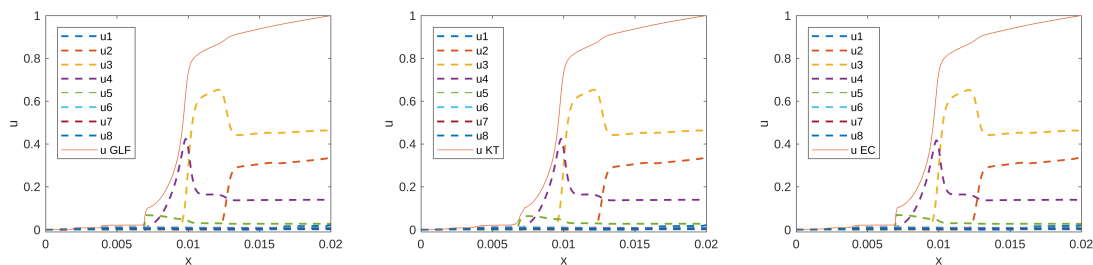


FIGURE 14. Example 5 (settling model, discontinuous degenerate diffusion, $N = 8$): comparison of numerical solutions computed using COMP-GLF, KT and EC ($\alpha = 1 \times 10^{-12}$) schemes, $M = 800$.

M	KT		COMP-GLF		EC($\alpha = 1.0 \times 10^{-12}$)	
	e_M^{tot}	θ_M	e_M^{tot}	θ_M	e_M^{tot}	θ_M
100	2.877e-4	—	9.554e-5	—	2.187e-4	—
200	1.345e-4	1.097	4.694e-5	1.025	1.027e-4	1.090
400	6.869e-5	0.969	2.872e-5	0.709	5.313e-5	0.951
800	3.882e-5	0.823	2.215e-5	0.375	2.202e-5	1.270
1600	2.332e-5	0.735	1.880e-5	0.237	8.378e-6	1.394

TABLE 6. Example 5 (settling model, discontinuous degenerate diffusion, $N = 8$): approximate L^1 errors (e_M^{tot}) and convergence rates (θ_M) at simulated time $t = 50$.

4.6. Example 5 (settling model, discontinuous degenerate diffusion, $N = 8$). In this example we consider the settling of dispersions of glycerol droplets of total initial concentration 50% in a column of biodiesel of depth $L = 20$ mm according to the experimental setup of [25]. The density of biodiesel is $\rho_c = 880$ kg/m³ and that of glycerol is $\rho_d = 1090$ kg/m³. Other parameters are the

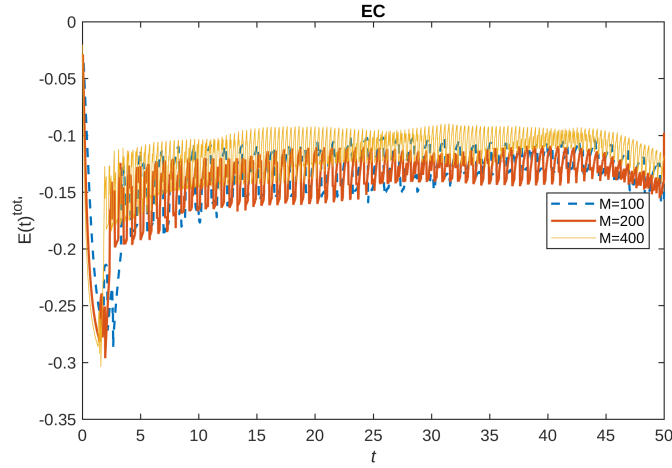


FIGURE 15. Example 5 (settling model, discontinuous degenerate diffusion, $N = 8$): $\tilde{\mathcal{E}}^{\text{tot},'}$ for EC ($\alpha = 1 \times 10^{-12}$) at different values of M .

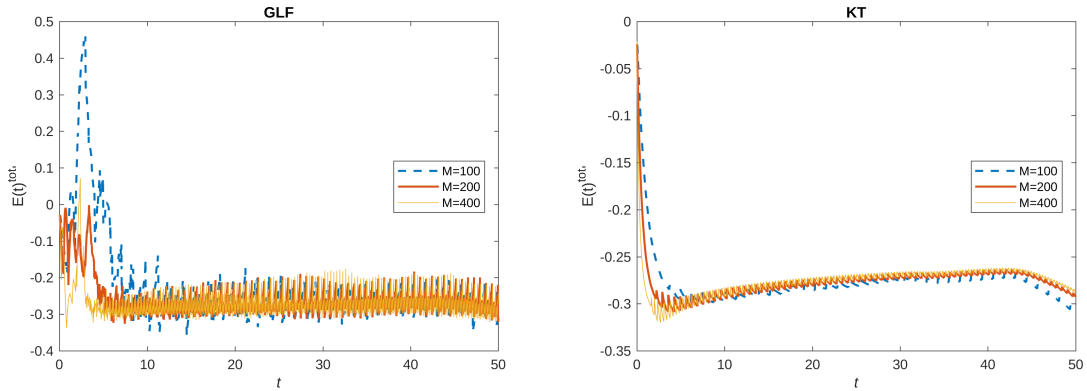


FIGURE 16. Example 5 (settling model, discontinuous degenerate diffusion, $N = 8$): $\tilde{\mathcal{E}}^{\text{tot},'}$ for GLF and KT Schemes at different values of M .

viscosity $\mu_c = 6.5$ m Pa and the diffusivity $D_0 = 10^{-7}$ m²/s. We consider $N = 8$ droplet size classes. The corresponding droplet diameters d_i and initial concentrations u_i^0 have been reconstructed from droplet size histograms [26], see Table 5. We also introduce a discontinuous diffusion function $\beta(u)$, namely

$$\beta(u) = \begin{cases} 0 & \text{if } u \leq u_c, \\ D_0 V(u) & \text{if } u > u_c, \end{cases}$$

where u_c is a critical density, or gel point, accounting for the onset of compression effects when entities of the disperse phase start forming permanent contact, for which we choose $u_c = 0.1$ in this example. Numerical results are obtained by the entropy stable (ES), component-wise global Lax-Friedrichs (COMP-GFL) and Kurganov-Tadmor (KT) schemes. Comparisons are made with results produced by the GLF-COMP Scheme, the reference solution is computed on a fine grid $M_{\text{ref}} = 6400$ (see Figure 13) and all methods are integrated in time by a SSPRK22 method with

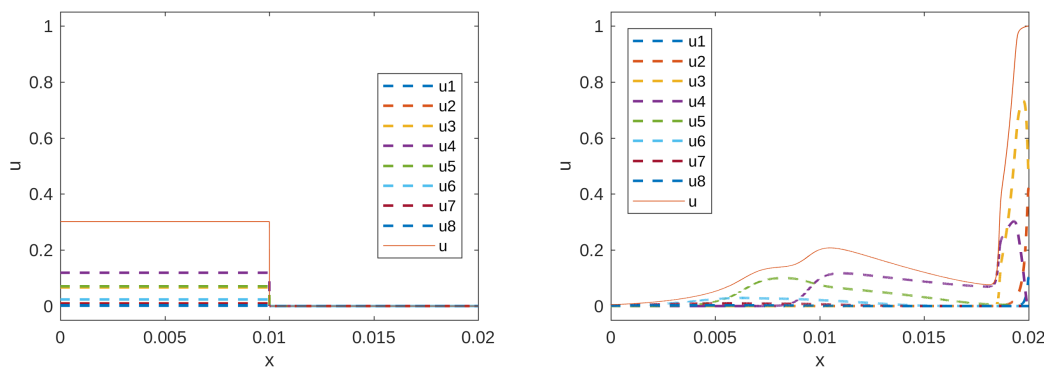


FIGURE 17. Example 6 (settling model, continuous diffusion, $N = 8$): (left) initial conditions and (right) reference solution computed with GLF Scheme and $M = 6400$ at $T = 200$.

	KT		COMP-GLF		EC($\alpha = 1.0 \times 10^{-12}$)	
M	e_M^{tot}	θ_M	e_M^{tot}	θ_M	e_M^{tot}	θ_M
50	3.5472e-4	—	2.7353e-4	—	3.7022e-4	—
100	2.4303e-4	0.546	2.2701e-4	0.269	2.8147e-4	0.395
200	1.9425e-4	0.322	2.1157e-4	0.102	2.1254e-4	0.405
400	1.7688e-4	0.136	2.0482e-4	0.047	1.7031e-4	0.320
800	1.7687e-4	0.000	2.0384e-4	0.007	1.5841e-4	0.105

TABLE 7. Example 6 (settling model, continuous diffusion, $N = 8$): approximate L^1 errors (e_M^{tot}) and convergence rates (θ_M) for Example 6 at simulated time $t = 200$.

$C_{\text{CFL}} = 0.3$. Observe that the numerical errors presented in Table 6, seem to indicate that the methods are not converging to the same solution. Qualitative results comparing the state of the system at end time, computed with each of the three methods are displayed in Figure 14.

For the present problem with its zero-flux boundary condition the growth of the total entropy is bounded by inequality (2.5), whose analogy for the semi-discrete entropy stable scheme is (2.20). To study whether the latter inequality is also valid in the fully discrete case, we plot for this and the next example (Figures 15 and 20, respectively) the quantity

$$\tilde{\mathcal{E}}_n^{\text{tot},'} := \frac{\Delta x}{\Delta t} \sum_{j=1}^M \left(\eta(\mathbf{u}_j^n) - \eta(\mathbf{u}_j^{n-1}) \right) + \varphi(\mathbf{u}_1^n) - \varphi(\mathbf{u}_M^n). \quad (4.8)$$

Note that, since $\varphi = \mathbf{v}^T \mathbf{f} - g$ after replacing (3.1) and (3.2), we have

$$\varphi(u) = \mathbf{v}(u)^T \mathbf{f}(u) - g(u) = \sum_{i=1}^N V(u) \frac{\log(u_i)}{v_i} v_i u_i - \left(V(u) \sum_{i=1}^N u_i \log(u_i) - \mathcal{V}(u) \right) = \mathcal{V}(u).$$

It is interesting to observe that contrary to the other two schemes, the component-wise global Lax-Friedrichs (COMP-GLF) scheme presents problems to preserve non-positivity of the quantity (4.8) at early stages of the time evolution process.

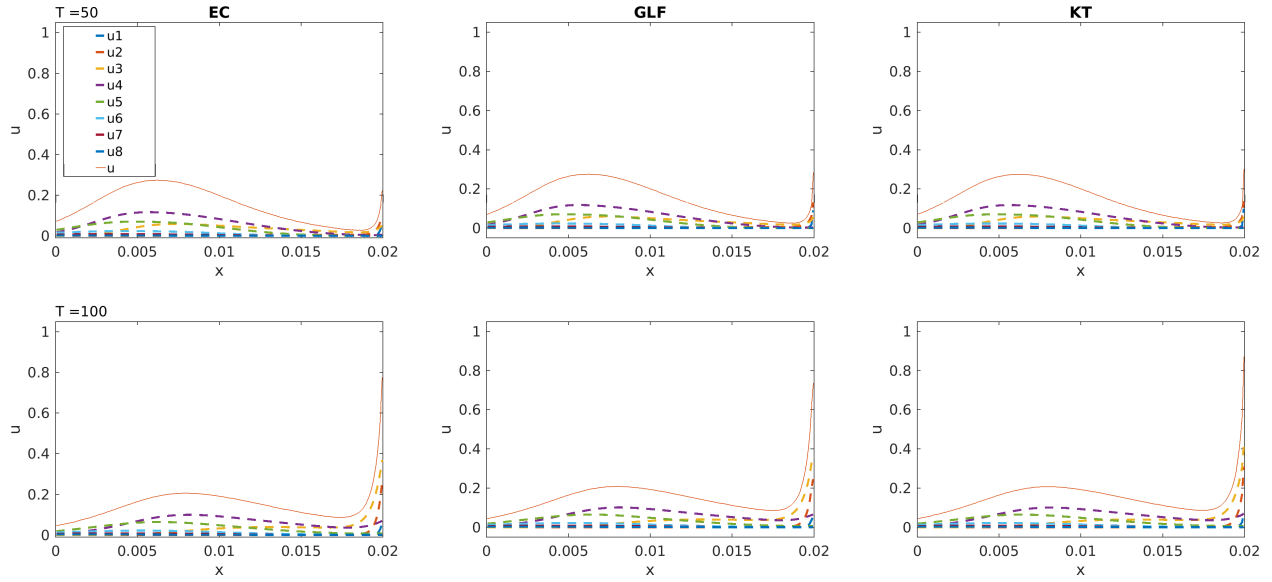


FIGURE 18. Example 6 (settling model, continuous diffusion, $N = 8$): numerical solutions at different times, $M = 200$.

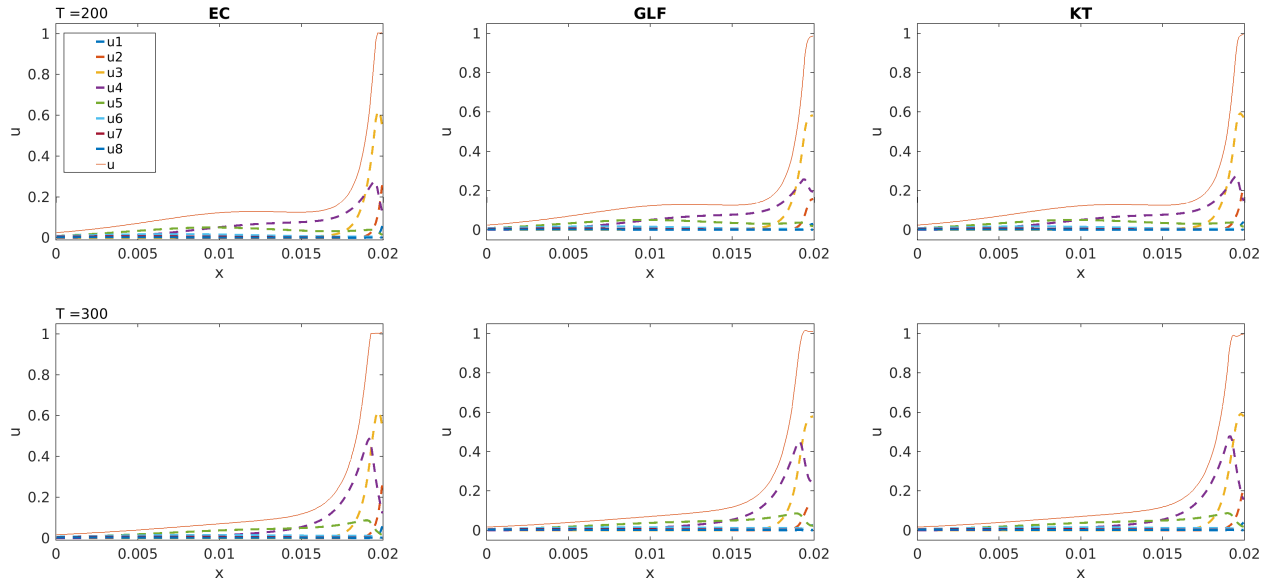


FIGURE 19. Example 6 (settling model, continuous diffusion, $N = 8$): numerical solutions at different times, $M = 200$.

4.7. Example 6 (settling model, continuous diffusion, $N = 8$). Now we consider the settling of a dispersion of 20% glycerol with a continuous diffusion function β . We suppose the initial concentration (scaled by a factor 1.5) is present only in the top half of the column as is shown in the left plot of Figure 17. Numerical approximations were computed using GFL, KT and EC schemes. In all cases $C_{CFL} = 0.1$ is used, and for the EC scheme a value $\alpha = 10^{-12}$ is chosen. Qualitative results comparing results for different times are shown in Figures 18 and 19.

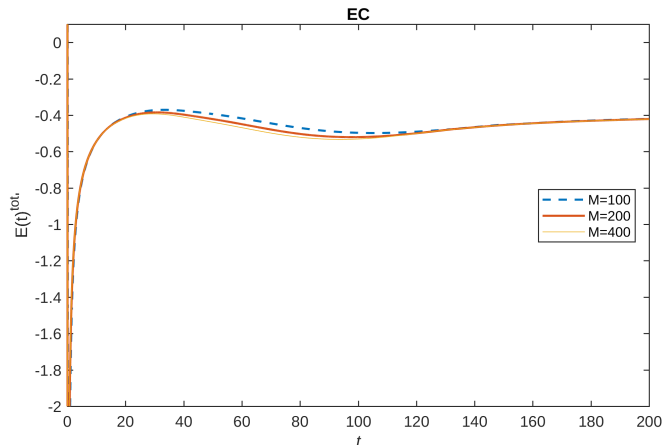


FIGURE 20. Example 6 (settling model, continuous diffusion, $N = 8$): $\tilde{\mathcal{E}}^{\text{tot},'}(t)$ for EC ($\alpha = 1 \times 10^{-12}$) at different values of M .

Numerical errors and convergence rates can be found on Table 7. All errors are computed against a numerical reference solution obtained with GFL scheme, CFL = 0.01 and a mesh of $M_{\text{ref}} = 6400$.

5. CONCLUSIONS

Entropy stable schemes for the numerical solution of initial value problems of nonlinear, possibly strongly degenerate systems of convection-diffusion equations proposed in [1] have been extended to initial-boundary value problems with zero-flux boundary conditions in one space dimension, including an explicit bound on the growth of the total entropy.

The numerical examples presented herein show that these schemes can be successfully used for the approximation of solutions in a class of diffusively corrected multiclass kinematic flow models. They also confirm the theoretical bounds for entropy in both cases, zero-flux boundary conditions and periodic boundary conditions. Furthermore, the results of Examples 2, 3 and 4 demonstrate that entropy stable schemes have a competitive computational efficiency compared with other common numerical schemes, when used on diffusively corrected multiclass kinematic flow models, like the traffic model and the polydisperse sedimentation model presented here. Although errors and errors rates are comparable with the other tested methods (Kurganov-Tadmor and component wise Global Lax Friedrichs) for coarser cell partitions, because of the differences on finer cell partitions we cannot entirely confirm that the methods converge to the same solution. This shortcoming is exacerbated by the lack of a well-posedness theory for (1.1) in the strongly degenerate case. It is therefore a topic requiring more careful study in future research.

We acknowledge that the current form of the schemes make them difficult to apply to more general real life problems. Their main limitation is the requirement of a diffusion matrix $\mathbf{K}(\mathbf{u})$ such that the product $\mathbf{K}\eta_{\mathbf{u},\mathbf{u}}^{-1}$ is positive definite, and the difficulty to obtain stable numerical fluxes from relation (2.21). We are currently investigating alternatives to relax these restrictions.

ACKNOWLEDGEMENTS

RB is acknowledges support by Fondecyt project 1170473; CONICYT/PIA/Concurso Apoyo a Centros Científicos y Tecnológicos de Excelencia con Financiamiento Basal AFB170001; and CRHIAM, project CONICYT/FONDAP/15130015. PM is supported by CONICYT scholarship

and SENESCYT scholarship. CP was partially supported by the Spanish Government and FEDER through the Research project MTM2015-70490-C2-1-R, and by the Andalusian Government through the project P11-FQM8179.

REFERENCES

- [1] S. Jerez, C. Parés, *Entropy stable schemes for degenerate convection-diffusion equations*, SIAM J. Numer. Anal. vol. 55 (2017) pp. 240–264.
- [2] E. Tadmor, *The numerical viscosity of entropy stable schemes for systems of conservation laws. I*, Math. Comp. vol. 49 (1987) pp. 91–103.
- [3] P.D. Lax, *Hyperbolic Systems of Conservation Laws and the Mathematical Theory of Shock Waves*, CBMS-NSF Regional Conf. Ser. in Appl. Math. vol.11, SIAM, Philadelphia, 1973.
- [4] M.J. Castro, U.S. Fjordholm, S. Mishra, C. Parés, *Entropy conservative and entropy stable schemes for nonconservative hyperbolic systems*, SIAM J. Numer. Anal. vol. 51 (2013) pp. 1371–1391.
- [5] U.S. Fjordholm, S. Mishra, E. Tadmor, *Energy preserving and energy stable schemes for shallow water equations with bottom topography*, J. Comput. Phys. vol. 230 (2011) pp. 5587–5609.
- [6] U.S. Fjordholm, S. Mishra, *Accurate numerical discretizations of non-conservative hyperbolic systems*, ESAIM: Math. Model. Numer. Anal. vol. 46 (2012) pp. 187–206.
- [7] U.S. Fjordholm, S. Mishra, E. Tadmor, *Arbitrarily high-order accurate entropy stable essentially nonoscillatory schemes for systems of conservation laws*, SIAM J. Numer. Anal. vol. 50 (2012) pp. 544–573.
- [8] A. Hildebrand, S. Mishra, *Entropy stable shock capturing spacetime discontinuous Galerkin schemes for systems of conservation laws*, Numer. Math. vol. 126 (2014) pp. 103–151.
- [9] R. Bürger, P. Mulet, L.M. Villada, *A diffusively corrected multiclass Lighthill-Whitham-Richards traffic model with anticipation lengths and reaction times*, Adv. Appl. Math. Mech. vol. 5 (2013) pp. 728–758.
- [10] R. Bürger, P. Mulet, L.M. Villada, *Regularized nonlinear solvers for IMEX methods applied to diffusively corrected multispecies kinematic flow models*, SIAM J. Sci. Comput. vol. 35 (2013) pp. B751–B777.
- [11] S. Boscarino, R. Bürger, P. Mulet, G. Russo, L.M. Villada, *Linearly implicit IMEX Runge-Kutta Methods for a class of degenerate convection-diffusion problems*, SIAM J. Sci. Comput. vol. 37 (2015) pp. B305–B331.
- [12] S.N. Kružkov, *First order quasilinear equations with several independent variables*, Mat. Sb. (N.S.) vol. 81 (1970) pp. 228–255.
- [13] J. Carrillo, *Entropy solutions for nonlinear degenerate problems*, Arch. Rational Mech. Anal. vol. 147 (1999) pp. 269–361.
- [14] S. Evje, K.H. Karlsen, *Monotone difference approximations of BV solutions to degenerate convection-diffusion equations*, SIAM J. Numer. Anal. vol. 37 (2000) pp. 1838–1860.
- [15] K.H. Karlsen, N.H. Risebro, J.D. Towers, *Upwind difference approximations for degenerate parabolic convection-diffusion equations with a discontinuous coefficient*, IMA J. Numer. Anal. vol. 22 (2002) pp. 623–664.
- [16] K.H. Karlsen, N.H. Risebro, *Convergence of finite difference schemes for viscous and inviscid conservation laws with rough coefficients*, M2AN Math. Model. Numer. Anal. vol. 35 (2001) pp. 239–269.
- [17] K.H. Karlsen, N.H. Risebro, *On the uniqueness and stability of entropy solutions of nonlinear degenerate parabolic equations with rough coefficients*, Discr. Contin. Dyn. Syst. vol. 9 (2003) pp. 1081–1104.
- [18] K.H. Karlsen, U. Koley, N.H. Risebro, *An error estimate for the finite difference approximation to degenerate convection-diffusion equations*, Numer. Math. vol. 121 (2012) pp. 367–395.
- [19] S. Benzoni-Gavage, R.M. Colombo, *An n -populations model for traffic flow*, European J. Appl. Math. vol. 14 (2003) pp. 587–612.
- [20] S. Benzoni-Gavage, R. Colombo, P. Gwiazda, *Measure valued solutions to conservation laws motivated by traffic modelling*, Proc. R. Soc. vol. 462 (2006) pp. 1791–1803.
- [21] R. Bürger, K.H. Karlsen, J.D. Towers, *On some difference schemes and entropy conditions for a class of multi-species kinematic flow models with discontinuous flux*, Netw. Heterog. Media vol. 5 (2010) pp. 461–485.
- [22] K. Stamatakis, C. Tien, *Batch sedimentation calculations—the effect of compressible sediment*, Powder Technol. vol. 72 (1992) 227–240.
- [23] R. Bürger, S. Diehl, M.C. Martí, P. Mulet, I. Nopens, E. Torfs, P.A. Vanrolleghem, *Numerical solution of a multi-class model for batch settling in water resource recovery facilities*, Appl. Math. Modelling vol. 49 (2017) pp. 415–436.
- [24] F. Rosso, G. Sona, *Gravity-driven separation of oil-water dispersions*, Adv. Math. Sci. Appl. vol. 11 (2001) pp. 127–151.

- [25] A. Abeynaïke, A.J. Sederman, Y. Khan, M.L. Johns, J.F. Davidson, M.R. Mackley, *The experimental measurement and modelling of sedimentation and creaming for glycerol/biodiesel droplet dispersions*, Chem. Eng. Sci. vol. 79 (2012) pp. 125–137.
- [26] R. Bürger, P. Mulet, L. Rubio, *Implicit-explicit methods for the efficient simulation of the settling of dispersions of droplets and colloidal particles*, Adv. Appl. Math. Mech. vol. 10 (2018) pp. 445–467.
- [27] R. Donat, F. Guerrero, P. Mulet, *Implicit-Explicit WENO scheme for the equilibrium dispersive model of chromatography*, Appl. Numer. Math. vol. 123 (2018) pp. 22–42.
- [28] R. Bürger, P. Mulet, L. Rubio, M. Sepúlveda, *Linearly implicit-explicit schemes for the equilibrium dispersive model of chromatography*, Appl. Math. Comput. vol. 317 (2018) pp. 172–186.
- [29] R.B. Lowrie, J.E. Morel, *Discontinuous Galerkin for Hyperbolic Systems with Stiff Relaxation*. In: Cockburn, B., Karniadakis, G.E., Shu, C.-W. (Eds.), Discontinuous Galerkin Methods. Lecture Notes in Computational Science and Engineering, vol 11. Springer, Berlin, Heidelberg. 2000.
- [30] U.S. Fjordholm, S. Mishra, E. Tadmor, *Arbitrarily high-order accurate entropy stable essentially nonoscillatory schemes for systems of conservation laws*, SIAM J. Numer. Anal. vol 50 (2012) pp. 544–573.
- [31] S. Gottlieb, C.-W. Shu, E. Tadmor, *Strong stability-preserving high-order time discretization methods*, SIAM Rev. vol. 43 (2001) pp. 89–112.
- [32] A. Kurganov, E. Tadmor, *New high-resolution central schemes for nonlinear conservation laws and convection-diffusion equations*, J. Comput. Phys. vol. 160 (2000) pp. 241–282.
- [33] G.C.K. Wong, S.C. Wong, *A multi-class traffic flow model—an extension of LWR model with heterogeneous drivers*, Transp. Res. A vol. 36 (2002) pp. 827–841.
- [34] M.J. Lighthill, G.B. Whitham, *On kinematic waves. II. A theory of traffic flow on long crowded roads*, Proc. Roy. Soc. London Ser. A vol. 229 (1955) pp. 317–345.
- [35] P.I. Richards, *Shock waves on the highway*, Oper. Res. vol. 4 (1956) pp. 42–51.
- [36] B.D. Greenshields, *A study of highway capacity*, Proc. Highway Res. Record, Washington, vol. 14 (1935) pp. 448–477.
- [37] F. Ismail, P.L. Roe, *Affordable, entropy-consistent Euler flux functions II: Entropy production at shocks*, J. Comput. Phys. vol. 228 (2009) pp. 5410–5436.
- [38] J.F. Richardson, W.N. Zaki, *Sedimentation and fluidization: Part I*, Trans. Instn. Chem. Engrs. (London) vol. 32 (1954) pp. 35–53.
- [39] A. Kurganov, S. Noelle, G. Petrova, *Semidiscrete central-upwind schemes for hyperbolic conservation laws and Hamilton-Jacobi equations*, SIAM J. Sci. Comput. vol. 23 (2001) pp. 707–740.

Centro de Investigación en Ingeniería Matemática (CI²MA)

PRE-PUBLICACIONES 2018

- 2018-13 RAIMUND BÜRGER, ENRIQUE D. FERNÁNDEZ NIETO, VICTOR OSORES: *A dynamic multilayer shallow water model for polydisperse sedimentation*
- 2018-14 ANTONIO BAEZA, RAIMUND BÜRGER, PEP MULET, DAVID ZORÍO: *Weno reconstructions of unconditionally optimal high order*
- 2018-15 VERONICA ANAYA, MOSTAFA BENDAHMANE, DAVID MORA, MAURICIO SEPÚLVEDA: *A virtual element method for a nonlocal FitzHugh-Nagumo model of cardiac electrophysiology*
- 2018-16 TOMÁS BARRIOS, ROMMEL BUSTINZA: *An a priori error analysis for discontinuous Lagrangian finite elements applied to nonconforming dual mixed formulations: Poisson and Stokes problems*
- 2018-17 RAIMUND BÜRGER, GERARDO CHOWELL, ELVIS GAVILÁN, PEP MULET, LUIS M. VILLADA: *Numerical solution of a spatio-temporal predator-prey model with infected prey*
- 2018-18 JAVIER A. ALMONACID, GABRIEL N. GATICA, RICARDO OYARZÚA, RICARDO RUIZ-BAIER: *A new mixed finite element method for the n-dimensional Boussinesq problem with temperature-dependent viscosity*
- 2018-19 ANTONIO BAEZA, RAIMUND BÜRGER, MARÍA CARMEN MARTÍ, PEP MULET, DAVID ZORÍO: *Approximate implicit Taylor methods for ODEs*
- 2018-20 RAIMUND BÜRGER, DANIEL INZUNZA, PEP MULET, LUIS M. VILLADA: *Implicit-explicit schemes for nonlinear nonlocal equations with a gradient flow structure in one space dimension*
- 2018-21 RICARDO OYARZÚA, MIGUEL SERÓN: *A divergence-conforming DG-mixed finite element method for the stationary Boussinesq problem*
- 2018-22 VERONICA ANAYA, AFAF BOUHARGUANE, DAVID MORA, CARLOS REALES, RICARDO RUIZ-BAIER, NOUR SELOULA, HECTOR TORRES: *Analysis and approximation of a vorticity-velocity-pressure formulation for the Oseen equations*
- 2018-23 ANA ALONSO-RODRIGUEZ, JESSIKA CAMAÑO, EDUARDO DE LOS SANTOS, FRANCESCA RAPETTI: *A graph approach for the construction of high order divergence-free Raviart-Thomas finite elements*
- 2018-24 RAIMUND BÜRGER, PAUL E. MÉNDEZ, CARLOS PARÉS: *On entropy stable schemes for degenerate parabolic multispecies kinematic flow models*

Para obtener copias de las Pre-Publicaciones, escribir o llamar a: DIRECTOR, CENTRO DE INVESTIGACIÓN EN INGENIERÍA MATEMÁTICA, UNIVERSIDAD DE CONCEPCIÓN, CASILLA 160-C, CONCEPCIÓN, CHILE, TEL.: 41-2661324, o bien, visitar la página web del centro: <http://www.ci2ma.udec.cl>



**CENTRO DE INVESTIGACIÓN EN
INGENIERÍA MATEMÁTICA (CI²MA)
Universidad de Concepción**



Casilla 160-C, Concepción, Chile
Tel.: 56-41-2661324/2661554/2661316
<http://www.ci2ma.udec.cl>

